

---

# Groundwater recharge in a sedimentary basin in semi-arid Mexico

Jürgen Mahlkecht · Jean F. Schneider ·  
Broder J. Merkel · Ignacio Navarro de León ·  
Stefano M. Bernasconi

**Abstract** Recharge mechanisms and the hydrochemical evolution of groundwater in a semi-arid, 6,840-km<sup>2</sup>, intermountain basin in central Mexico were investigated using stable isotopes and major chemical constituents. Ionic ratio analysis helped to conceptualize and quantify in part the subsequent geochemical evolution in the aquifer system. Mass balance models (PHREEQC) were used to interpret and rectify the geochemical properties of the aquifer. The recharge conditions have not changed noticeably during the last several thousands of years. The recharge mechanisms are accompanied by leaching of meteoric salts on and near the ground surface during

major rain events, which previously accumulated after minor rain events. Rapid and diffuse infiltration can be excluded. Indirect infiltration from wadis (arroyos) and depressions (playas) with little mixing in shallow groundwater contrasts with a high degree of mixing for water with deep circulation. The prevailing source of major cations (Ca<sup>2+</sup>, Mg<sup>2+</sup>, Na<sup>+</sup>, K<sup>+</sup>) is weathering of carbonates and albite, followed by exchange reactions on clays and hydroxides. Ca<sup>2+</sup>/Na<sup>+</sup> exchange may interchange along the flow path with reverse (Na<sup>+</sup>/Ca<sup>2+</sup>) exchange, although the Ca<sup>2+</sup>/Na<sup>+</sup> option is prevalent. Meteoric Ca and Mg inputs are relatively small; however, meteoric Na is insignificant. Irrigation return flow plays an important role in the western part of the study area, giving rise to elevated sulfate and chloride concentrations.

---

Received: 24 September 2002 / Accepted: 27 February 2004  
Published online: 20 July 2004

© Springer-Verlag 2004

---

J. Mahlkecht (✉)  
Institute of Applied Geology,  
Universität für Bodenkultur Wien,  
Peter Jordan-Strasse 55, 1190 Wien, Austria  
e-mail: jurgen@quijote.ugto.mx  
Tel.: +52-473-7321813  
Fax: +52-473-7323535

J. F. Schneider  
Institute of Applied Geology,  
Universität für Bodenkultur Wien,  
Peter Jordan-Strasse 55, 1190 Wien, Austria

B. J. Merkel  
Department of Geology,  
Technische Universität Bergakademie Freiberg,  
Gustav Zeunerstrasse 12, 09596 Freiberg, Germany

I. Navarro de León  
Facultad de Ciencias de la Tierra,  
Universidad Autónoma  
de Nuevo León Ex-Hacienda de Guadalupe,  
Carr. Linares-Cerro Prieto km. 8,  
67700 Linares, Nuevo León, Mexico

S. M. Bernasconi  
Institute of Geology, Eidgenössische Technische Hochschule,  
ETH-Zentrum, 8092 Zurich, Switzerland

*Present address:*

J. Mahlkecht, Facultad de Ingeniería en Geomática e Hidráulica,  
Universidad de Guanajuato,  
Avenida Juárez 77, Zona Centro, CP 36000, Mexico

**Résumé** Les mécanismes de recharge et l'évolution hydrochimique de l'eau souterraine dans un bassin de montagne de 6 840 km<sup>2</sup> en zone semi-aride, dans le centre du Mexique, ont été étudiés au moyen des isotopes stables et des composés chimiques majeurs. L'analyse des rapports ioniques a aidé à conceptualiser et à quantifier en partie l'évolution géochimique qui en résulte, dans le système aquifère. Des modèles de bilan de masse (PHREEQC) ont été utilisés pour interpréter et corriger les propriétés de l'aquifère. Les conditions de recharge n'ont pas changé notablement au cours des derniers millénaires. Les mécanismes de recharge sont accompagnés, durant les épisodes majeurs de précipitation, d'un lessivage, à la surface du sol et à son voisinage, de sels météoriques accumulés auparavant pendant les petits épisodes de pluie. L'infiltration rapide et diffuse peut être exclue. L'infiltration indirecte à partir des oueds (arroyos) et des dépressions (playas) avec un faible mélange dans la nappe superficielle contraste avec le degré élevé de mélange de l'eau avec les circulations profondes. La source prépondérante des cations majeurs (Ca<sup>2+</sup>, Mg<sup>2+</sup>, Na<sup>+</sup>, K<sup>+</sup>) est l'altération des carbonates et des feldspaths ; l'échange de cations avec les argiles et les hydroxydes est moins important. L'échange de Ca<sup>2+</sup> avec Na<sup>+</sup> peut s'inverser le long des axes d'écoulements pour donner un échange de Na<sup>+</sup> avec Ca<sup>2+</sup>, bien que le cas Ca<sup>2+</sup>/Na<sup>+</sup> soit prépondérant. Les apports météoriques de Ca et de Mg sont relativement faibles, cependant que celui de Na météorique est insignifiant. L'écoulement par retour d'irrigation joue un rôle important dans la partie occi-

dentale de la région étudiée, produisant un accroissement des concentrations élevées en sulfate et en chlorure.

**Resumen** Se han investigado los mecanismos de recarga y la evolución hidroquímica de las aguas subterráneas en una cuenca semiárida e intermontana de México central, de 6.840 km<sup>2</sup>. Para ello, se han utilizado isótopos estables y los constituyentes químicos mayores. El análisis de las relaciones iónicas ha servido para conceptualizar y cuantificar en parte su evolución geoquímica posterior dentro del sistema acuífero. Se ha recurrido a modelos de balance de masas (PHREEQC) para interpretar y rectificar las propiedades geoquímicas del acuífero. Las condiciones de recarga no han cambiado de forma apreciable durante los últimos miles de años. Los mecanismos de recarga se ven acompañados por el lixiviado de las sales meteóricas sobre y cerca de la superficie del terreno durante los episodios principales de lluvia, las cuales son acumuladas en episodios menores de lluvia. Se puede excluir la infiltración rápida y difusa. La infiltración indirecta desde arroyos (*wadis*) y depresiones (*playas*), que apenas se mezcla con las aguas subterráneas someras, contrasta con un elevado nivel de mezcla con el agua de circulación profunda. La fuente dominante de cationes mayores (calcio, magnesio, sodio, potasio) es la meteorización de los carbonatos y albita, mientras que las reacciones de intercambio en las arcillas e hidróxidos son menos importantes. El intercambio ión calcio-ión sodio puede ser reemplazado a lo largo de una línea de flujo por el intercambio opuesto (ión sodio-ión calcio), aunque la primera es prioritaria. Las aportaciones meteóricas de calcio y magnesio son relativamente pequeñas, mientras que la de sodio es insignificante. Los retornos de riego desempeñan un papel importante en la parte occidental del área de estudio, dando lugar a concentraciones elevadas de sulfato y cloruro.

**Keywords** Semi-arid regions · Groundwater recharge · Stable isotopes · Hydrochemistry · Mexico

## Introduction

More than half of Mexico is located in the Mexican Highlands (Altiplano) with arid and semi-arid climatic conditions. This area receives less than 20% of the nation's precipitation while containing 75% of the 97 million inhabitants, 70% of the industrial and 40% of the agricultural activity, respectively, of the country (CNA 1995). In recent years, the water demand of these sectors has grown, causing water balance deficits of 20% in the aquifers. Because of the scarcity of surface water in this region, the population greatly depends on groundwater resources. The competition for the groundwater threatens the water resources, with the subsequent generation of environmental, economic and socio-economic problems. According to the Comisión Nacional del Agua (CNA), from the 459 aquifers under survey, 32 were overex-

ploited in 1975, 36 in 1981, 80 in 1985, and 100 in 1999 (CNA 2000).

Groundwater management in semi-arid and arid regions in central and northern Mexico, however, is often faced with the difficult task of explaining the origin, evolution and renewability of groundwater in aquifers prone to overexploitation. The reasons are insufficiency of hydrological, geophysical and hydrochemical data, and an often complex aquifer system with horizontal and vertical groundwater flow components.

In the extensively developed Independence Basin (6,840 km<sup>2</sup>) in the Altiplano (Fig. 1) there is a heavy demand for agricultural, domestic, commercial, and industrial water supplies. Accelerated development of groundwater resources over the past three decades has resulted in a severe decline of potentiometric levels. This region in the Guanajuato State is known to be one of the most extensively exploited in Mexico.

Nowadays more than 2,500 active water extraction wells exist in the study area extracting in 1980, in 1991 and in 2000 about 412, 542, and 700 million m<sup>3</sup>/year, respectively (SARH 1981; CNA 1992; CODEREG 2000). Agriculture uses around 63% of the total extraction volume. The average water level decline in wells of the western and eastern part of the study area is 0.8 and 1.2 m/year, respectively (CEAG 2001). Currently, the mean static water table in the center of the basin averages about 80 m below ground level (CEASG 1999). Groundwater withdrawn from the deepest portion is up to 13,000 years old, based on radiocarbon dating (Mahlknecht 2003). The exploitation of paleogroundwater has also been reported in other regions of the Mexican Altiplano (e.g. Payne et al. 1971; Carrillo-Rivera et al. 1992, 1996; Edmunds et al. 2002). The most prominent and maybe the most complicated overexploited aquifer in Mexico underlies the metropolitan area of Mexico City (Birkle et al. 1998; Edmunds et al. 2002).

Due to an increasing tendency of groundwater reservoir exploitation in the valley, the knowledge of the recharge rates and characteristics has become an important issue to safeguard a sustainable use of groundwater resources. This study uses isotopic and chemical signatures of water to identify recharge magnitude and processes, and ionic ratios and numerical models to trace the geochemical evolution of groundwater. Ionic ratio analyses are nowadays often replaced by standard computer programs (e.g. Parkhurst et al. 1982; Plummer et al. 1991; Parkhurst 1995), but are still in use. They are useful to conceptualize the groundwater geochemistry of a study area and to corroborate and constrain computer models, since computer solutions frequently offer non-unique solutions, requiring a modeler to understand the geochemistry and hydrogeology to decide which of the available models are most feasible.

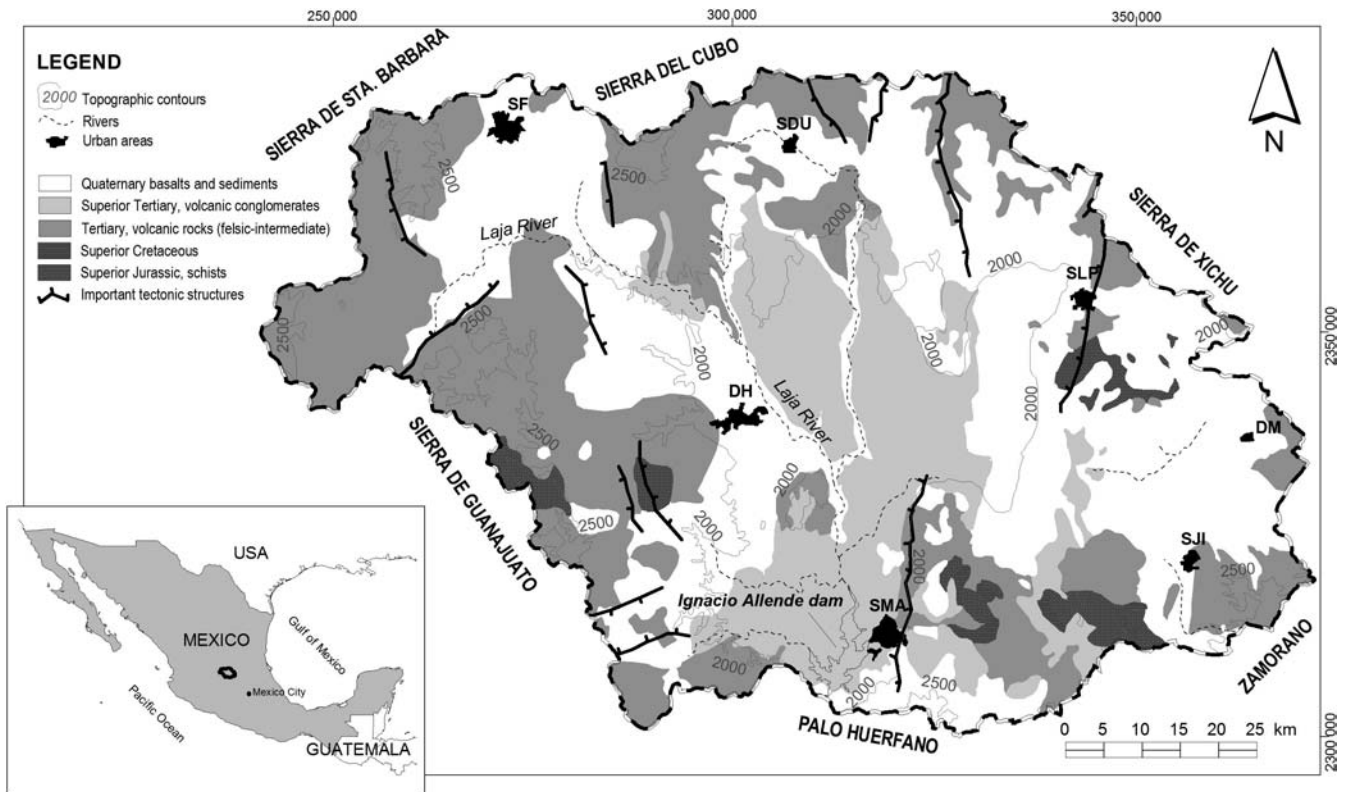


**Fig. 1** Location of the Independence Basin study area with general surficial geologic and topographic features and towns (*DH* Dolores Hidalgo; *DM* Doctor Mora; *SLP* San Luis de la Paz; *SDU* San Diego de la Unión; *SF* San Felipe; *SJI* San José de Iturbide; *SMA*

San Miguel de Allende). Topographic contours in meters above sea level. The used projection system is Universal Transverse Mercator System

## Theory

### Chloride Mass Balance Method

The chloride mass balance (CMB) method for the estimation of groundwater recharge is economic and effective. The conditions for a successful application of the CMB method according to Wood (1999), are: (1) atmospheric chlorine is the only source for chloride in groundwater, (2) chloride behaves as a conservative tracer along the flow path, (3) chloride uptake by roots and anion exclusion are negligible, (4) leaching of chlorine-containing strata at ground surface and in the soil zone is complete, (5) groundwater movement in both unsaturated zone and saturated zone can be approximated by one-dimensional piston flow, and (6) surface run-on and runoff can be neglected. Thus, if the amount of precipitation  $P$  and the effective chloride concentration of surface infiltration resulting from wet and dry deposition ( $C_{eff}$ ) and chloride concentration of groundwater ( $C_{GW}$ ) are known, the mass balance approach can be used to estimate recharge flux  $R$ :

$$R = P \frac{C_{eff}}{C_{GW}}$$

Although erroneously assuming a steady-state condition, and violating some of the numerous assumptions when it is applied in the saturated zone (e.g. one-dimen-

sional piston flow), this conventional approach and other reliable methods (Scanlon et al. 2002; Zhu et al. 2003) are very useful for a first approximation of the recharge flux estimation in semi-arid and arid regions, specially due to the lack of hydrological data.

### Isotopic Composition of Water During Recharge Processes

Since  $^{18}\text{O}$  and  $^2\text{H}$  in water behave chemically conservatively below 60–80 °C (Issar and Gat 1981), their concentrations are not affected by geochemical reactions in normal aquifers (Hoefs 1997). Therefore, groundwater preserves its isotopic fingerprint reflecting the history and origin before infiltration. This makes it a useful tool to interpret recharge mechanisms. With respect to Craig's relationship (Craig 1961), the long-term arithmetic mean for all stations of the International Atomic Energy Agency (IAEA) network is:  $\delta^2\text{H} = (8.17 \pm 0.06) \delta^{18}\text{O} + (10.35 \pm 0.65)$  (Rozansky et al. 1993). The last term of the equation, the deuterium excess (d-value), can vary locally, primarily as a function of the vapor-forming process. For central Mexico the regional d-value is +11.03 (Cortés et al. 1997).

Isotope fractionation is strongly dependent on the temperature. A significant correlation between the mean annual concentrations of stable isotopes in precipitation

and mean annual air temperature is likely to be observed (Daansgard 1964). This knowledge has found application in the identification of recharge during paleo-climatic periods (e.g. Mazor and Verhagen 1983; Darling et al. 1997), distant mountain recharge (e.g. Clark et al. 1987) or seasonality of recharge in temperate regions (e.g. Rozansky et al. 1982).

On the other hand, large rain events are more depleted in isotopic composition than small rain events, due to the preferential rainout of heavy isotopes. This effect is intensified by the enrichment of heavy isotopes, due to evaporation during minor rain events (Levin et al. 1980). Evaporation process alters the original  $^{18}\text{O}$ - $^2\text{H}$  relationship of the rainfall resulting in d-values lower than eight, as reported in many arid regions (Gat 1980). During the evaporation of water from the surface or soil water, enrichment of  $^{18}\text{O}$  and  $^2\text{H}$  occurs.

### Sources of Chloride Salinity in Natural Waters

If variations in chloride concentrations in natural waters are due to mixing of meteoric water with recent or formational water in buried marine sediments, then the  $\delta^{18}\text{O}:\text{Cl}$  ratio values of groundwater should be positively correlated and plot on a mixing line between the composition of seawater and that of the least saline groundwater (Payne 1988). If salinity is due to the enrichment of salts by evaporation, then the  $^{18}\text{O}$ - $^2\text{H}$  signature would have a low slope reflecting kinetic fractionation. In addition, a plot of chloride content against either isotope  $^{18}\text{O}$  or  $^2\text{H}$  will be positively correlated, as increased evaporation would result in isotopic enrichment as well as an increased chloride concentration (Payne 1988). If transpiration is the predominant concentration mechanism, then the  $^{18}\text{O}$ - $^2\text{H}$  signature will have a slope similar to that of the regional rainfall, as transpiration results in no significant isotope fractionation (Allison et al. 1984). The chloride vs. isotope relationship would then define a line with a steep slope, as there would be little variation in isotopic content with increasing salinity. If salinity is due to the leaching of evaporitic salts by rapid percolation through preferential pathways, then the groundwater should retain an  $^{18}\text{O}$ - $^2\text{H}$  relationship similar to that of regional rainfall. As the leaching process does not affect the isotopic composition of water, there would be no correlation between isotope content and chloride concentration (Payne 1988). Finally, if chemical weathering is the primary source of dissolved salts, then the anion and cation concentrations of specific salts should be correlatable, with increasing concentrations along the flowpath (Rosenthal 1987). Furthermore, if marine formation salts and halite deposits (e.g. by means of fertilizers, waste water etc.) can be excluded so that chloride is solely of meteoric origin, the abundance of chloride compared with other ions can be used as an index of the relative contribution of meteoric salts to those resulting from mineral weathering.

## Study Area

### General Description

The Independence Basin in the Central Mexican Altiplano is an intermountain sedimentary basin with a surface area of about 6,840 km<sup>2</sup>, with the lowest elevations of 1,850 m above sea level (a.s.l.) and summits of 2,850 m a.s.l. Dolores Hidalgo, San Miguel de Allende, San José Iturbide, San Felipe, and San Diego de la Unión, are important settlements in the valley. The total population is about 500,000. The main stream, the Laja River, originates south of San Felipe and leaves the basin west of San Miguel de Allende at the southern border of the study area (Fig. 1). The stream discharge contributes to the Lerma–Chapala–Santiago river system which ends up in the Pacific Ocean. The basin is named after the Mexican independence battle against the Spanish conquerors in 1820, having its historical origins in the center of the basin. Dolores Hidalgo is regarded as the “Cradle of the Independence”.

The current climate in the area is semi-arid according to the definition of UNESCO (1979), with a mean annual precipitation (monitored from 1961 to 2001 at 21 meteorological stations) <400 mm in the plains and >800 mm in the highlands. The rainfall season is from May to October, with 35 to 86 mm/month. The range of precipitation during the dry season from November to April is from 8 to 18 mm/month, February being the driest month. The mean annual temperature and the mean summer temperature are 17.1 and 21.0 °C, respectively, (climatic data from Servicio Meteorológico Nacional).

From the edaphological point of view (FAO-UNESCO 1988), the study area is predominantly haplic to luvic feozem in the center and the north, and pelic vertisol in the south (between Dolores Hidalgo and San Miguel de Allende) of the study area. Haplic xerosol (San Felipe) and calcic cambisol (San Luis de la Paz) are of local significance. A typical phenomenon of soils in some parts of the study area (e.g. Mineral de Pozos) is the accumulation of calcium carbonate (*caliche*) immediately beneath the solum.

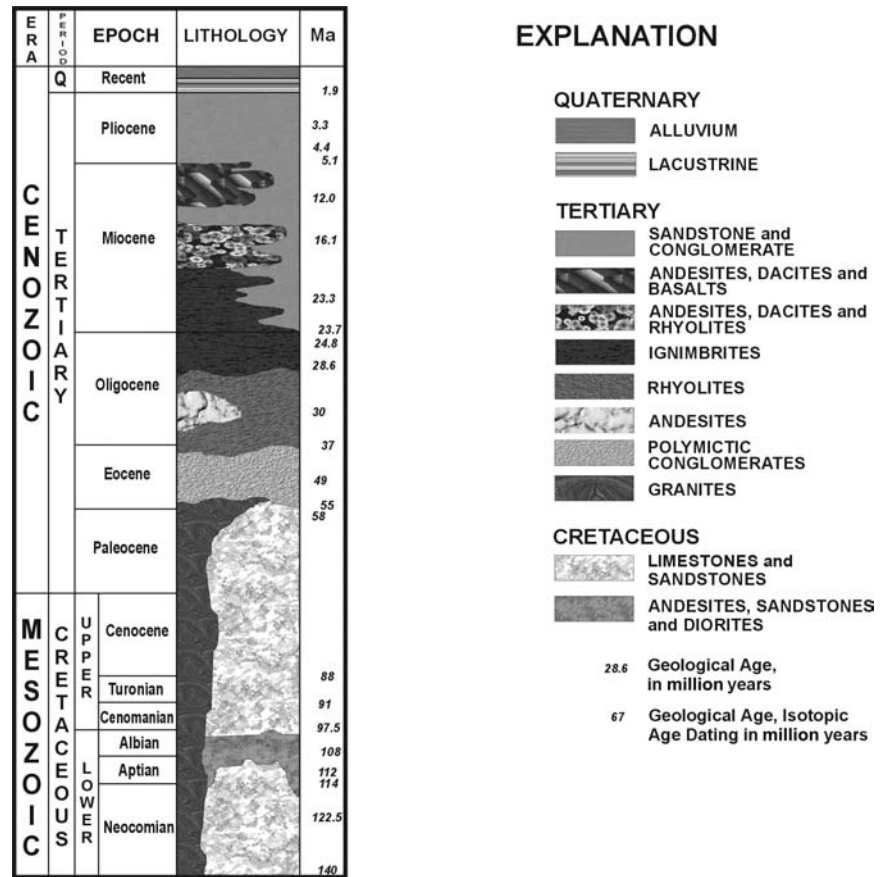
### Geologic and Hydrogeologic Settings

The study area constitutes the southern border of the Mexican Basin and Range province (Aranda-Gómez and McDowell 1998). The geological framework, shown in Fig. 1, indicates the volcano-sedimentary nature of the study area. Hydrogeology, lithology and stratigraphy are documented in CNA (1992), CEASG (1999), and CODEREG (2000). Groundwater heads in wells are recorded biannually by the Comisión Estatal del Agua de Guanajuato (CEAG) since 1999.

Mineralogical data from several investigations were summarized by Mahlke (2003). According to this review, volcanic rocks consist of albite (range from 8 to 42 wt%), K-mica (0–37%), K-feldspar (0–30%), plagioclase (0–27%), anorthite (0–34%) and quartz (0–24%). Sediments include quartz (0–30%), albite (0–32%), feld-



**Fig. 2** Chronostratigraphic column for the Independence Basin; modified from CODEREG (2000)



spar (0–25%), kaolinite (0–13%), Ca-montmorillonite (0–12%), hematite (1–6%) and calcite (0–2%). Sandstones contain mainly quartz, feldspar and rock fragments. Anorthite is found mainly in basaltic Quaternary formations in the south (San Miguel de Allende) and northeast (San Luis de la Paz) of the study area, whereas Ca-montmorillonite, chalcedony and kaolinite are only present in downgradient aquifer zones (toward the basin's center and the Ignacio Allende Dam).

The hydrogeologic characteristics of the catchment area are interpreted based on the concept of tensional stresses provoking the differential settling of tectonic blocks, and simultaneously filling these grabens with thick layers of volcanoclastic sediments (Aranda-Gómez and McDowell 1998; Ferrari et al. 1999). The lithological units which crop out in the study area can be divided into: (1) the basal limestone, sandstone and granite complex of the Early Cretaceous Period, and the (2) cover complex of the Cenozoic Era of mainly felsic to intermediate volcanic and sedimentary rocks, and derived sediments (Fig. 2).

From the hydrogeological point of view, the upper part of the aquifer consists of alluvial to lacustrine sandy to silty sediments, interstratified with volcanic conglomerates and tuffs, and in the lower unit of sandstones and fractured ignimbrites of mainly rhyolitic origin. The median of transmissivity of the upper alluvial to lacustrine layer is  $4.0 \times 10^{-3} \text{ m}^2/\text{s}$  (Mahlknecht 2003).

The total groundwater recharge volume in the study area according to a water mass balance approach, is 170 million  $\text{m}^3/\text{year}$  (CNA 1992). Groundwater discharge to streams and springs is thought to be depreciable at the present time, due to the relatively deep groundwater table in most of the basin and the decreasing number of springs. However, much evidence exists that the pre-1960 groundwater table was shallow (i.e. less than 20 m below ground level), such as depleted springs, relicts of shallow wells (*norias*) and former lakes (*lagunas*) (CODEREG 2000). This indicates possibly important effects of evaporation in the past. Evaporation at the present time is enhanced by the commonly used ditch irrigation system. Figure 13 presents the present-day water table configuration (1999).

Actual evapotranspiration in the study area after Turc's method (Gray 1973), is 518 mm/year. The Coutagne method (Remenieras 1974) results in an average of 449 mm/year. The potential evapotranspiration after Blaney-Criddle (Blaney 1959) is 1,280 mm/year. The potential runoff according to the SCS runoff curve numbers proposed by the US Soil Conservation Service (SCS 1964) is calculated as 33.7 mm/year for the western, and 34.3 mm/year for the eastern part of the study area (CEASG 1999).

## Materials and Methods

### Field and Laboratory Methods

Forty-six groundwater samples were collected from agricultural and domestic water production wells from April to June 2000 (Mahlknecht 2001). The chemical data was completed with a set of 200 samples from a previous study (CODEREG 2000) which was collected from March to May 1999. The methods of sampling and laboratory procedures for both studies were the same (see below). For some boreholes sampled in both collection periods and compared, there were no significant differences in chemical composition.

The anion and cation samples were filtered (0.45  $\mu\text{m}$ ) and stored with tri-distillate water, in new pre-rinsed HDPE bottles (Nalgene) at a constant temperature of 4 °C. Additionally, cation samples were acidified to a pH <2 by ultrapure nitric acid (Baker). The cations and anions were determined by Activation Laboratories Ltd. in Ancaster, Ontario, with inductive-coupled plasma mass spectrometry (ICP-MS) and ion chromatography, respectively. In cases where sodium concentrations exceeded 25 mg/L, sodium concentrations were determined by mass balance calculation and/or ICP-OES (inductively coupled plasma optical emission spectroscopy).

A flow-through cell (5 L) with low constant flow of water was used to perform the field measurements. pH was determined with a pH-mV meter with temperature electrode (model "pH196", WTW). Prior to any readings, the pH meter was calibrated with reference buffer solutions of pH 7 and 4 (or 10). The specific electrical conductance (EC) and temperature were taken by an EC meter (model "LF 191", WTW). Alkalinity determination was completed in the field by titration with 1.5 N  $\text{H}_2\text{SO}_4$  and Methyl orange (Hycel).

Seventy-eight water samples were analyzed for stable isotopes at the Isotope Laboratory of the University of Waterloo, Canada, and reported by CODEREG (2000). Analyses for  $^{18}\text{O}$  and  $^2\text{H}$  are expressed in  $\delta$ -notation relative to Vienna standard mean ocean water (VSMOW) standards.

Twenty-one rainwater samples were collected from the meteorological station at Dolores Hidalgo between April 2000 and April 2002 for chemical analysis. The analyses are reported in Mahlkecht (2003).

### Interpretation

Recharge fluxes were estimated locally by application of the chloride mass balance (CMB) method and regionalized by interpolation. Groundwater chloride data for 246 sample sites were used together with distributed precipitation rate and the mass-weighted average of 21 chloride concentration values from rain events at Dolores Hidalgo between April 2000 and April 2002.

In order to distinguish between different origins of groundwater, a non-hierarchical cluster analysis (K-means) was applied with stable isotope data to determine groups in a matrix with similar characteristics. Since

cluster analysis does not offer an internal statistical check for significance, a post-hoc analysis of variables was applied to compare the means. The Bonferroni adjustment method (Winer et al. 1991) and a confidence level of 5% were used. All statistical analyses were performed using the SPSS program (SPSS 1999). The results were proved for geographical correspondence with geologic/geomorphologic features.

The geochemical evolution and dissolution rates were identified and estimated by both phenomenological analyses and numerical geochemical modeling. The phenomenological analyses used an ionic ratio calculation according to a scheme developed by Sami (1992). Since chloride in the Independence aquifer water is of meteoric origin and salinization effects other than halite dissolution can be excluded, this chemical constituent could be used as a qualitative means to differentiate between waters of different residence times.

In order to evaluate species, saturation indices, and mass transfers in the water-rock system, the geochemical code PHREEQC (Parkhurst and Appelo 1999) was used. The mass transfers were calculated for samples along several flow paths. The corresponding samples were chosen taking into account the geographical position of the sampling point, the hydraulic-head distribution of the aquifer system and observed hydrochemical trends (chloride increase along flowpath). The global uncertainty used for ion concentrations was 5%. The individual uncertainty for some ions (K, Na, Ca) was increased to 20% in some cases, where necessary. The database phreeqc.dat was used for all calculations and the reactants were selected based on potential reactions between water and the investigated mineral phases.

## Results

### Recharge Fluxes

According to a water mass balance approach, the total amount of recharge in the study area is 170 million  $\text{m}^3$ /year or 24.9 mm/year (CNA 1992). CEASG (1999) reported recharge estimates via runoff curve numbers according to the US Soil Conservation Service (SCS 1964). According to this method, the plains in the northern part receive no infiltration. The chloride mass balance (CMB) method applied in the present study used mean annual precipitation (30-year records), chloride concentrations from 246 wells, and chloride concentrations of rainfall (rain events from a two-year period). According to this approach, the recharge rate was calculated as 171 million  $\text{m}^3$ /year, with minima in the plains of the northern study area (10 mm/year; San Diego de la Unión) and maxima in the southeastern mountainous area (>800 mm/year; Sierra de Guanajuato) (Fig. 3). The map shows the geographical correspondence of the recharge and precipitation distribution. This approach also shows that the intermittent Laja River does not contribute a significant amount of basin recharge (Fig. 3). The results demonstrate also that the estimates by the

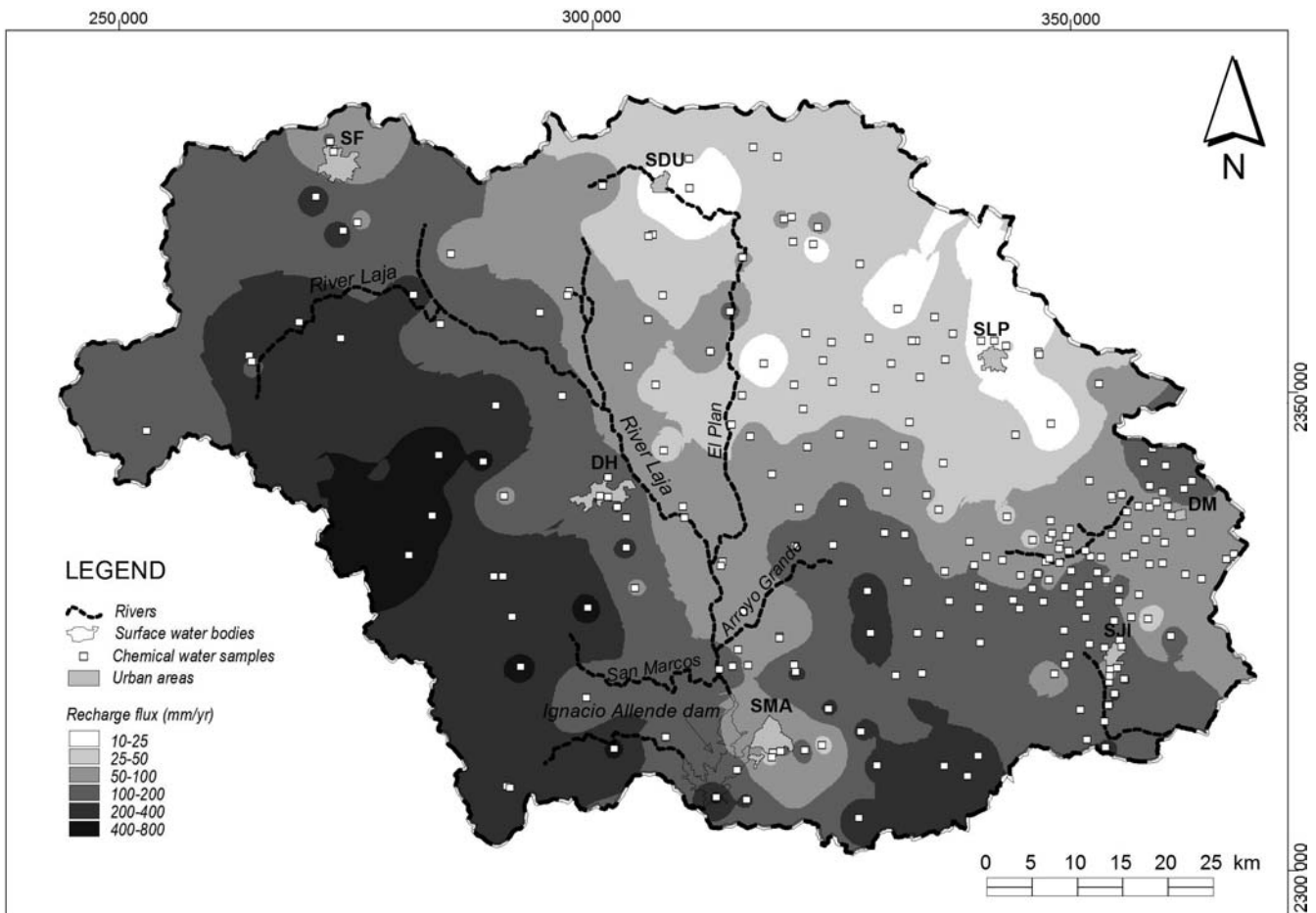


Fig. 3 Recharge flux distribution calculated by the chloride mass balance method

CMB method are lower than those obtained from the SCS method.

### Isotopic Results

The  $\delta^{18}\text{O}$  and  $\delta^2\text{H}$  data vary between  $-12.7$  and  $-6.8\text{‰}$ , and  $-92.2$  and  $-57.2\text{‰}$  VSMOW, respectively. The corresponding average values are  $-10.0 \pm 0.9\text{‰}$  and  $-73.5 \pm 6.4\text{‰}$ . The mean isotopic concentration of the rainwater from which the groundwater was derived suggests that the mean  $^{18}\text{O}$  of rainfall events resulting in recharge is about  $-12.7\text{‰}$  VSMOW (Fig. 4). This value corresponds to the most isotopically depleted groundwater samples, and represents therefore the largest rainfall events in the region and/or groundwater infiltrated at higher elevations. The most enriched groundwater ( $-6.8\text{‰}$ ) represents lower elevations and/or short rainfall events.

The isotopic data was divided into three homogeneous types by using the deuterium excess and the K-means algorithm (Fig. 5). Type 1 is represented by  $\delta^2\text{H} = 6.97 \delta^{18}\text{O} - 4.40$  ( $n = 39$ ,  $R^2 = 0.91$ ). Type 2 can be fitted by  $\delta^2\text{H} = 8.04 \cdot \delta^{18}\text{O} + 11.84$  ( $n = 27$ ,  $R^2 = 0.89$ ) and is situated mainly at the eastern portion of the study basin, whereas type 3 is represented by the regression curve of  $\delta^2\text{H} = 8.35 \cdot \delta^{18}\text{O} - 16.80$  ( $n = 12$ ,  $R^2 = 0.90$ ), and represents

the western portion of the watershed area (Fig. 5). The regression line of type 2 fits nicely with the regional meteoric water line (RMWL) developed by Cortés et al. (1997) for the basin of Mexico City and surroundings ( $\delta^2\text{H} = 7.97 \cdot \delta^{18}\text{O} + 11.03$ ), and the global meteoric water line. Type 3, on the other hand, shows a distinct regression line, which most likely represents precipitation of a different origin, i.e. from rainstorms coming from the Atlantic Ocean and rainfall in the mountainous zone of the western part of the study area (Sierra de Guanajuato) (Fig. 5). Type 1, represents a mixture between types 2 and 3. Type 3 and 1 imply impact by evaporation effects. The samples of these types correspond to the water in the majority of wells in the farmlands (Fig. 5).

### Hydrochemical Results

The mass-weighted average chemical composition of rainwater from 21 rain events is:  $\text{Ca} = 0.39$  mg/L;  $\text{Mg} = 0.05$  mg/L;  $\text{K} = 0.41$  mg/L;  $\text{Na} = 0.28$  mg/L;  $\text{Cl} = 0.16$  mg/L;  $\text{SO}_4 = 1$  mg/L; and  $\text{NO}_3 = 0.1$  mg/L. Detailed analyses are reported in Mahlkecht (2003).

The pH of groundwater ranges between 5.3 and 9.2 with an average of 7.3 and a standard deviation of 0.5. A

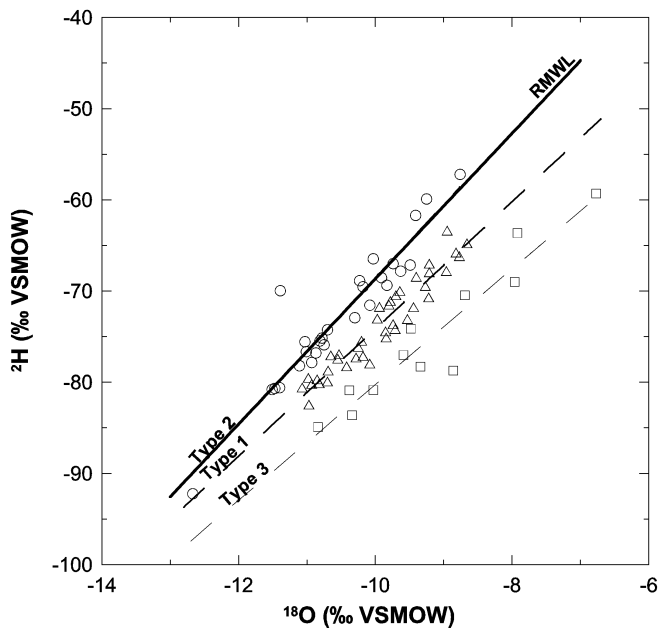


**Fig. 4** Relationship between  $\delta^2\text{H}$  and  $\delta^{18}\text{O}$  in groundwater of the Independence catchment. *RMWL* Regional mean water line; *Dashed lines* indicate regression lines for each group

summary of the water properties and chemical constituents is given in Table 1.

The waters are listed according to their content of major cations and anions by using the Piper diagram (Fig. 6). Those from the recharge zones fall predominantly in the category of  $\text{Ca}^{2+}\text{-HCO}_3^-$  to  $\text{Ca}^{2+}\text{-Na}^+\text{-HCO}_3^-$  type with a pH of 6 to 8. In the downgradient zones, the groundwater is of the  $\text{Na}^+\text{-Ca}^{2+}\text{-HCO}_3^-$  type with a pH as high as 9.

The average value for total dissolved solids (TDS) is  $443 \pm 202$  mg/L. Two samples from the eastern part of the study area (Mineral de Pozos mining district area) fall in the category of  $\text{Ca}^{2+}\text{-SO}_4^{2-}$  with elevated mineralization (TDS=1,700 mg/L), which may originate from a mixture with water from the lower confined Cretaceous limestone formation (Fig. 1). These waters are only of local importance and not used for drinking, and thus they are not considered in the following discussion.

Saturation indices from groundwater samples from the Independence aquifer reveal that water is generally undersaturated with respect to albite, chalcedony, amorphous silica, gypsum and halite; variably saturated with K-feldspar, and supersaturated with kaolinite. A general progressive trend from unsaturated to a saturated state

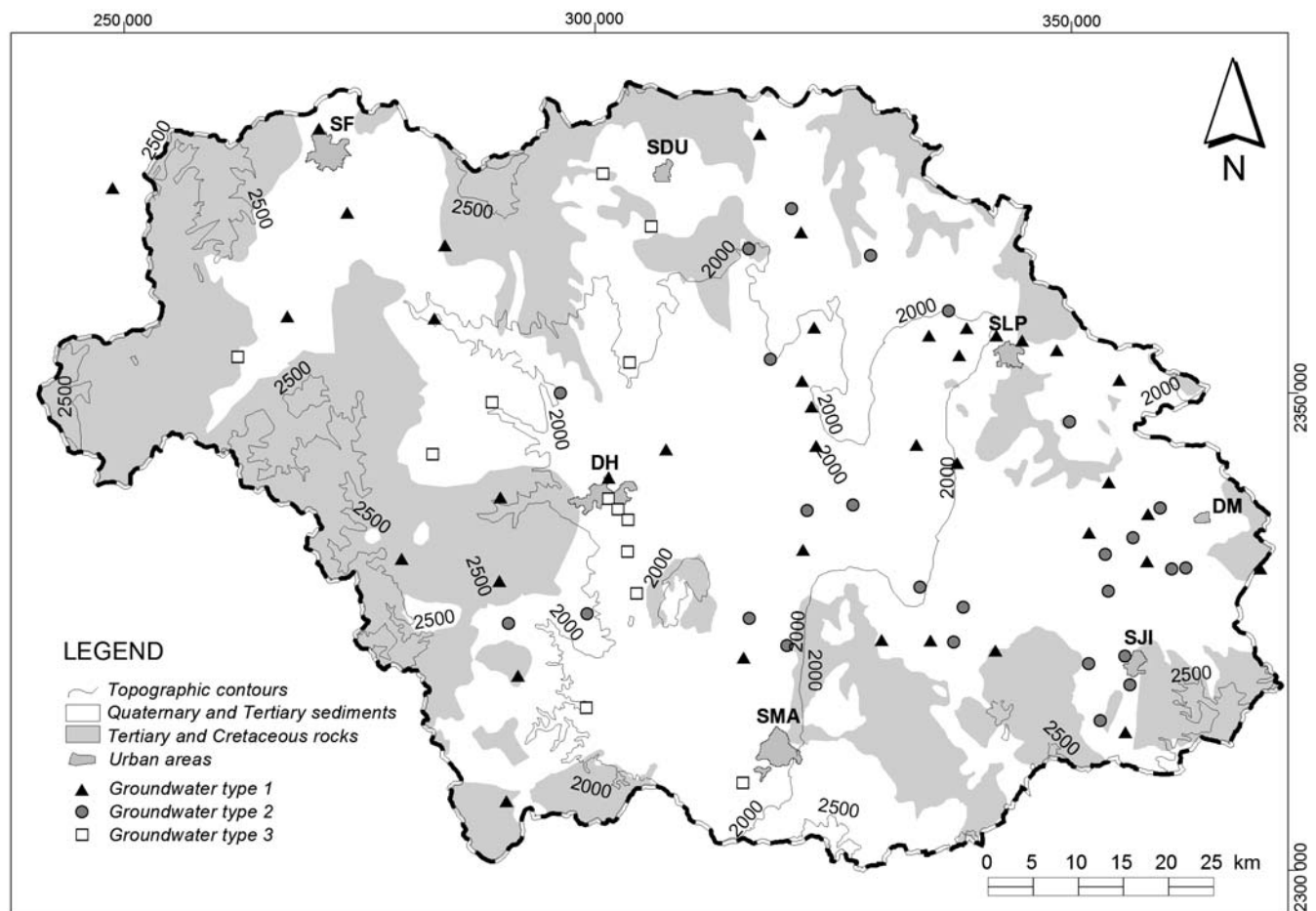


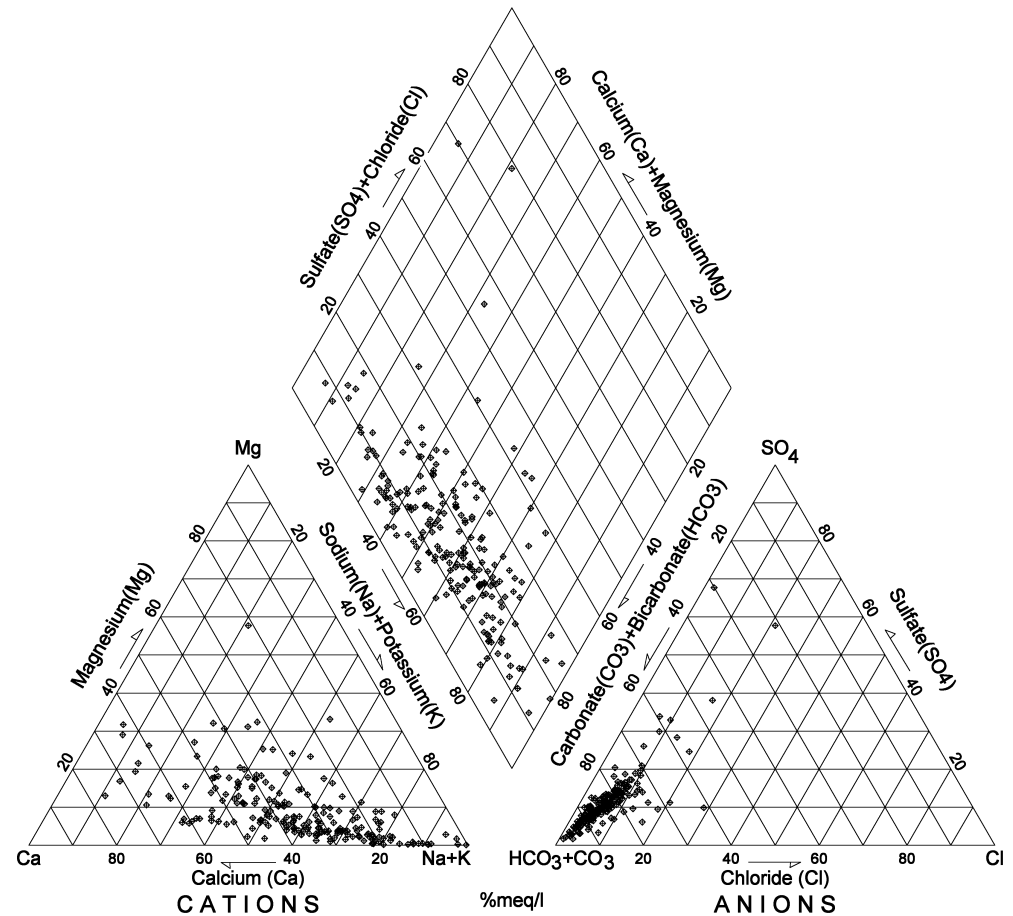
**Fig. 5** Study area showing distribution of groundwater types based on stable isotope values. Elevation of topographic contours; meters ASL



**Table 1** Summary of water properties and chemical constituents (in mg/L, except otherwise indicated). E.C. means electrical conductivity

	No.	Minimum	Maximum	Mean	Std. Deviation
Temperature (°C)	246	14.2	47.4	27.2	5.1
pH	246	5.3	9.2	7.3	0.51
E.C. ( $\mu\text{S}/\text{cm}$ at 25°C)	246	40.0	1,999.0	486.0	201.1
Na	246	0.7	293.9	54.3	33.6
K	246	0.9	73.0	13.7	8.0
Ca	246	0.7	315.0	36.8	30.5
Mg	246	0.02	96.6	6.3	8.4
SiO <sub>2</sub>	246	14.6	138.2	71.1	23.5
HCO <sub>3</sub>	246	11.9	738.0	251.9	86.9
Cl	246	1.2	65.0	10.5	9.3
NO <sub>3</sub>	246	0.0	295.0	3.4	18.8
SO <sub>4</sub>	246	1.2	835.0	30.1	63.0

**Fig. 6** Piper diagram for definition of groundwater chemical types



occurs along the evolutionary path. This trend is observed especially with the more reactive phases such as calcite and dolomite. Groundwater evolves from highly undersaturated to undersaturated states with respect to halite and gypsum. This suggests that the presence of dissolved chloride is limited by halite or meteoric chloride (Fig. 7).

## Discussion

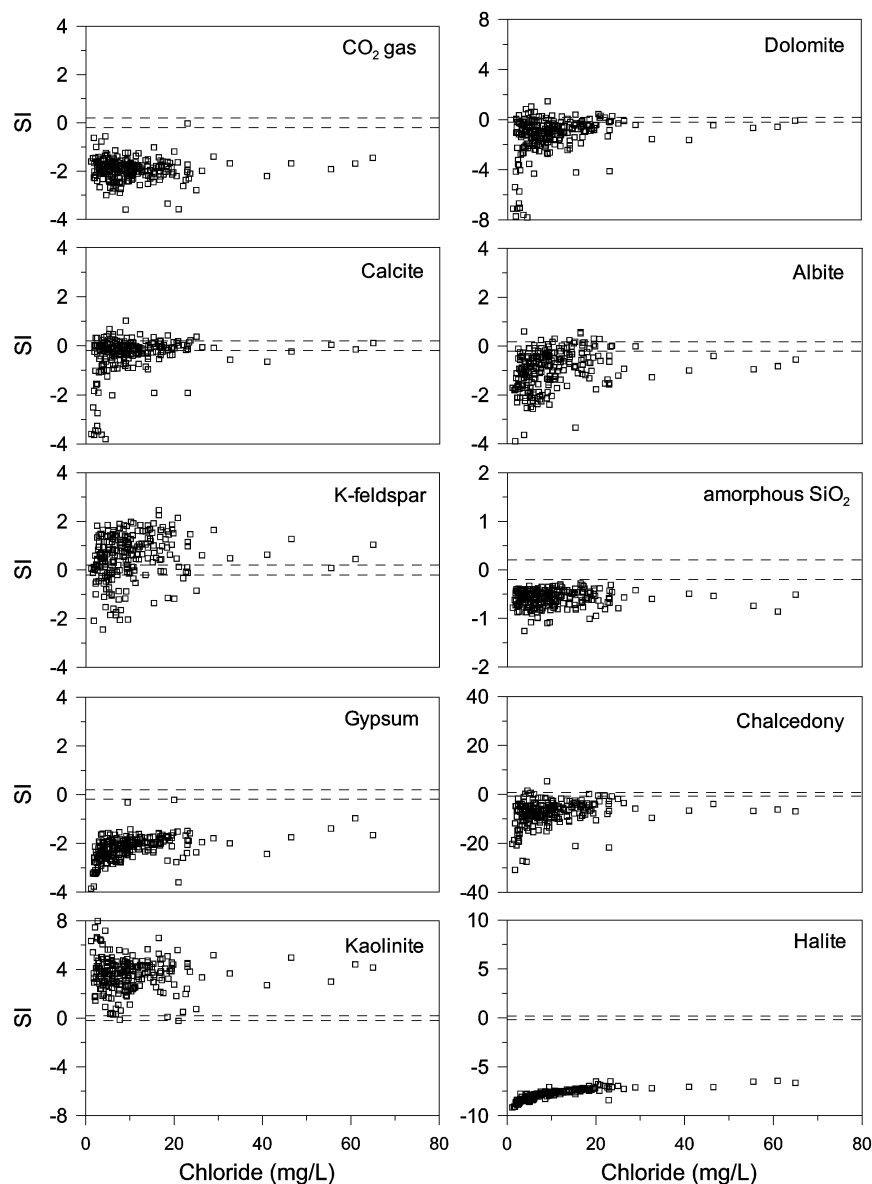
### Recharge Processes

Groundwater  $^{18}\text{O}$ - $^2\text{H}$  relationships do not intersect with the seawater composition. Furthermore, increases in

chloride concentration are not attributed to isotopic enrichment (Fig. 8A), which indicates that the presence of chloride is ascribed to meteoric accumulation.

Figure 5 implies that evaporation effects correspond to intensively cultivated farmlands where recirculation by irrigation water is an important factor. Salt accumulated at the surface from short rainfall events is episodically re-dissolved and leached into the groundwater during heavy rainfall and irrigation events, both being isotopically depleted. However, Fig. 8A indicates that the evaporative enrichment does not produce significant salinity increases. The fact that  $^{18}\text{O}$  and chloride are not correlated significantly may suggest that the concentration of salts by

**Fig. 7** Saturation indices and log partial pressure of CO<sub>2</sub> gas versus chloride concentration, according to speciation-solubility calculations



evaporation is not an important process in the Independence Basin.

Low infiltration rates and frequent overland flow indicate that diffuse recharge is not very likely. The probable recharge mechanism obtained from the isotopic evidence and field observations, is indirect recharge from wadis (*arroyos*) and surface depressions (*playas*) with cyclic drying (isotopic enrichment) and wetting (concentration of salts). The accumulation of chloride occurs in the first 40 m of depth of the water table below ground level as indicated by groundwater samples from farmlands with known groundwater levels in the northern part of the study area (Fig. 9). An explanation for high chloride contents in shallow- and intermediate-depth water could be a high evapotranspiration rate resulting from agricultural irrigation. In addition, the intensive use of fertilizers, which frequently contain chlorine, could reach the groundwater table. On the other hand, deep ground-

water below intensively cultivated agricultural lands is not yet affected by this return flow. Assuming return flow moves down at 1.5 m/year and the depth to groundwater is 80 m, then the return flow would reach groundwater in about 50 years. The additional chloride originating from agriculture has further implications for the applicability of the CMB analytical results regarding recharge in farmlands in the northern part of the study area. The recharge estimates from the intensively cultivated farmlands are probably too low.

The <sup>18</sup>O and <sup>2</sup>H contents are a function of a variety of atmospheric conditions such as temperature, distance from vapor source, and rates of evaporation. Additional modifications are due to subsurface processes, such as mixing. From Fig. 8B, it can be seen that the  $\delta^{18}\text{O}$  values of springs and shallow groundwater (depth to water table <20 m) and intermediate-depth are similar distributed, a further indication of preferable indirect infiltration for

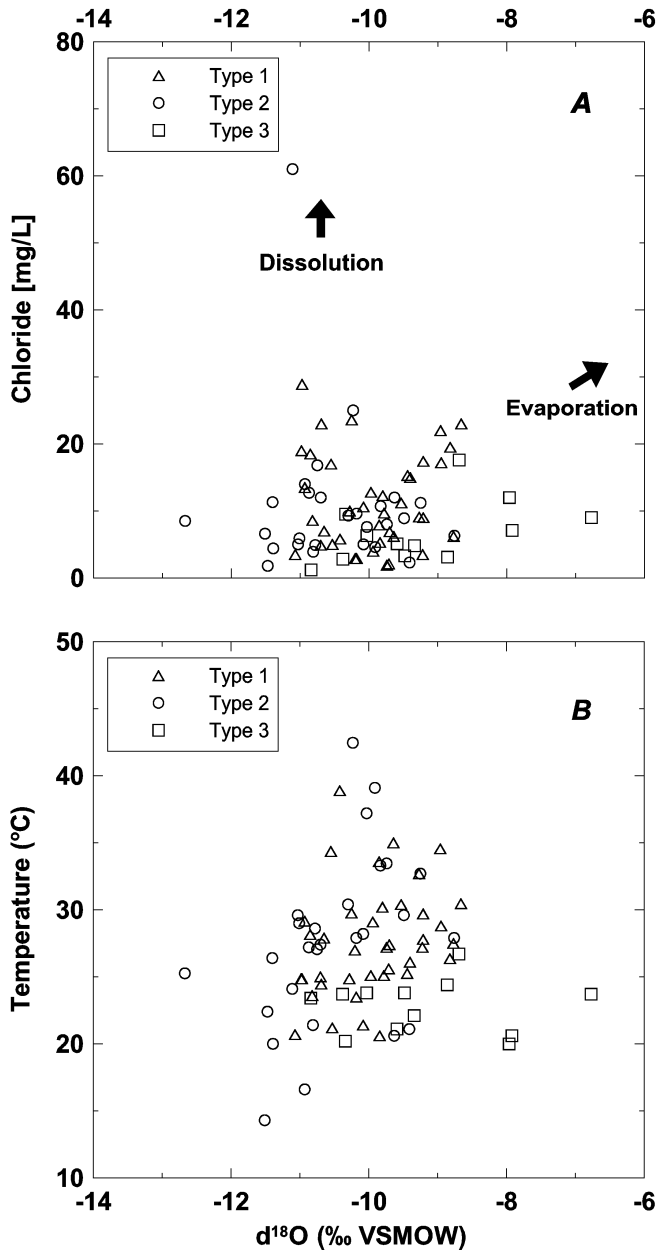


**Fig. 8** A Relationship between chloride and  $\delta^{18}\text{O}$  in groundwater; B  $\delta^{18}\text{O}$  as function of temperature for groundwater and springs. The deeper groundwater converges on the mean value of  $-10.1\text{‰}$

shallow and intermediate water. Carrillo-Rivera et al. (1992), however, showed a different condition in a similar catchment of the Altiplano, 70 km north of the present study area. These authors found that the isotope content of shallow water is considerably dispersed in comparison to deep water, reflecting direct recharge and minimal evaporative effects at depth.

While the  $\delta^{18}\text{O}$  content of shallow groundwater varies from  $-7$  to  $-13\text{‰}$ , it converges with growing temperature/depth on the value of  $-10.1\text{‰}$  (Fig. 8B). Lesser variations indicate longer flow paths with hydrodynamic dispersion and mixing smoothing seasonal and spatial variations. The mean value coincides with the mean value of shallow

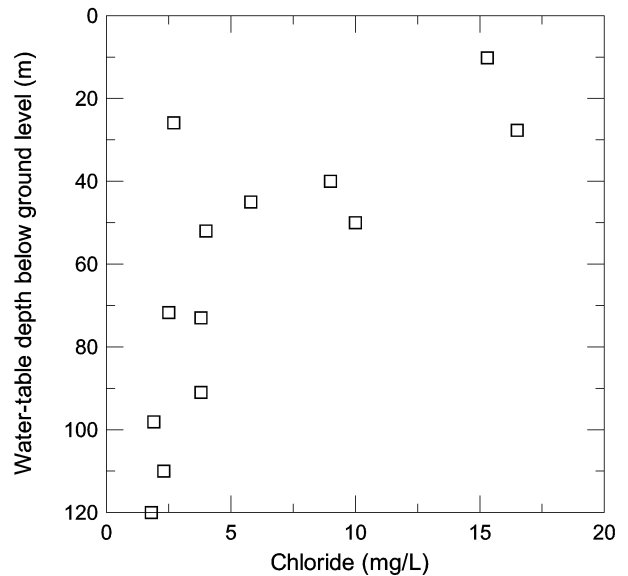


**Fig. 9** Chloride concentration as a function of water table depth for intensively cultivated farmlands

water varying within the standard deviation of spring water. Likewise, in other groundwater studies in the Mexican Altiplano (Issar et al. 1983; Carrillo-Rivera et al. 1992, 1996), temperature can be used as an indication of depth of groundwater circulation. Since Issar et al. (1983) show that the meteoric relationship of paleogroundwaters is similar to that observed in modern groundwater from the Mexican Altiplano, the similarity of shallow and deep groundwater can be taken as indirect evidence for similar recharge conditions.

**Geochemical Evolution**

The cyclic wetting and drying processes described in the isotopic interpretation can be affirmed by using the relationship between sulfate and chloride. The groundwater samples contain sulfate in the expected amount from simple evaporation of rainfall (as indicated by the 1:1 plot in Fig. 10). This shows that percolating water dissolves completely all highly soluble halite and less soluble salts (gypsum). In dry regions it is often observed that groundwater samples contain less sulfate than would be expected from simple evaporation due to only partial dissolution of gypsum during the percolation of soil water (Drever 1997). In the Independence Basin, however, the infiltration processes are obviously slow enough to obtain equilibrium with several minerals (e.g. gypsum).

Ionic ratios of groundwater samples were compared to determine whether any subsequent evolution of water chemistry occurs. Table 2 indicates that calcium and magnesium, and calcium and sulfate are significantly correlated suggesting that precipitation of  $\text{CaCO}_3$  is not a significant process for calcium losses.

The Na/Cl ratio ranges from 48.6 to 0.2, in general diminishing with growing salinity (Fig. 11A). Apparently, this water does not mix with seawater or groundwater

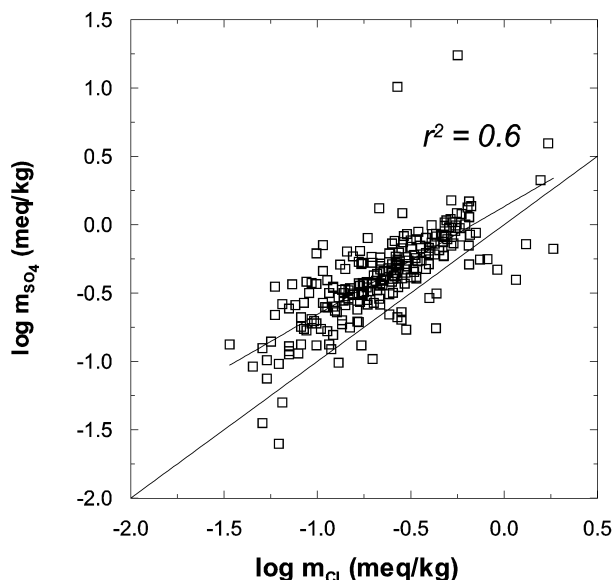
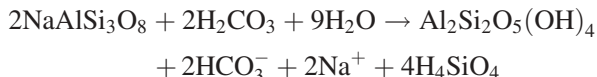


Fig. 10 Sulfate vs. chloride concentrations in groundwater

from halite deposit dissolution. Na/Cl ratios in excess of 1.0 at low salinities imply that meteoric NaCl is not the only source of sodium. Incongruent feldspar weathering occurs, readily releasing sodium and kaolinite according to the albite weathering reaction:



Another reason for elevated sodium concentrations at low salinities can be cation exchange processes in the aquifer where clay particles exchange calcium and magnesium against sodium. Calcium and magnesium are therefore depleted relative to  $\text{HCO}_3^-$ . Most potential lithological sources of calcium and magnesium result in  $(\text{Ca}+\text{Mg})/\text{HCO}_3^-$  ratios of 0.5 (see below); however, at low salinities, the  $(\text{Ca}+\text{Mg})/\text{HCO}_3^-$  ratios are less than 0.5 (Fig. 11B). The low  $(\text{Ca}+\text{Mg})/\text{HCO}_3^-$  ratios could be the result of either calcium or magnesium depletion by cation exchange, chlorite dissolution, or bicarbonate enrichment due to silicate weathering. The Na/Cl ratio declines with increasing salinity which suggests that cation exchange processes pick up sodium in exchange for bounded calcium (and magnesium in lesser amounts), thereby depleting sodium while enriching the calcium (and magne-

sium) concentrations in solution with respect to bicarbonate.

The Mg/Ca ratio varies between 2.23 and 0.01 (Fig. 11C); however, no trend can be found. Recall from Table 2 that only a small part, or none, of calcium is possibly depleted by  $\text{CaCO}_3$  precipitation. The differences of magnesium and calcium compared to chloride are therefore attributed mainly to exchange of sodium against calcium and magnesium and weathering processes. The scattering in Fig. 11C indicates also that magnesium derives rather from magnesium containing silicates than from dolomite.

The  $(\text{Mg}+\text{Ca})/\text{HCO}_3^-$  ratio explains the sources of calcium and magnesium in groundwater. All  $(\text{Mg}+\text{Ca})/\text{HCO}_3^-$  ratios of the present study with the exception of two samples are found to be lower than 0.5 (Fig. 11B). The ratio increases with salinity which implies that Mg and Ca are being added to the solution at a greater rate than bicarbonate. If magnesium and calcium originate solely from weathering of carbonates in the aquifer cement [ $\text{CaCO}_3+\text{H}_2\text{O}+\text{CO}_2\rightarrow\text{Ca}^{2+}+2\text{HCO}_3^-$ ], dolomite [ $\text{CaMg}(\text{CO}_3)_2+2\text{H}_2\text{O}+2\text{CO}_2\rightarrow\text{Mg}^{2+}+\text{Ca}^{2+}+4\text{HCO}_3^-$ ] or magnesite [ $\text{MgCO}_3+\text{H}_2\text{O}+\text{CO}_2\rightarrow\text{Mg}^{2+}+2\text{HCO}_3^-$ ], this ratio would be about 0.5. If chlorite [ $\text{Mg}_5\text{Al}_2\text{Si}_3\text{O}_{10}(\text{OH})_8+16\text{H}^+\rightarrow5\text{Mg}^{2+}+2\text{Al}^{3+}+3\text{H}_4\text{SiO}_4+6\text{H}_2\text{O}$ ] or biotite dissolution [ $\text{KMg}_3\text{AlSi}_3\text{O}_{10}(\text{OH})_2+6\text{H}^++4\text{H}_2\text{O}\rightarrow\text{K}^++3\text{Mg}^{2+}+\text{Al}(\text{OH})_4^-+3\text{H}_4\text{SiO}_4$ ] is the main source of alkalis, the ratio would be lower. Chlorite and biotite dissolution may, however, not be important due to the lower dissolved magnesium concentration in comparison to calcium (Fig. 11C). Mineralogical findings in southern zones of the study area show that anorthite dissolution is a possible contributor to the dissolved calcium content.

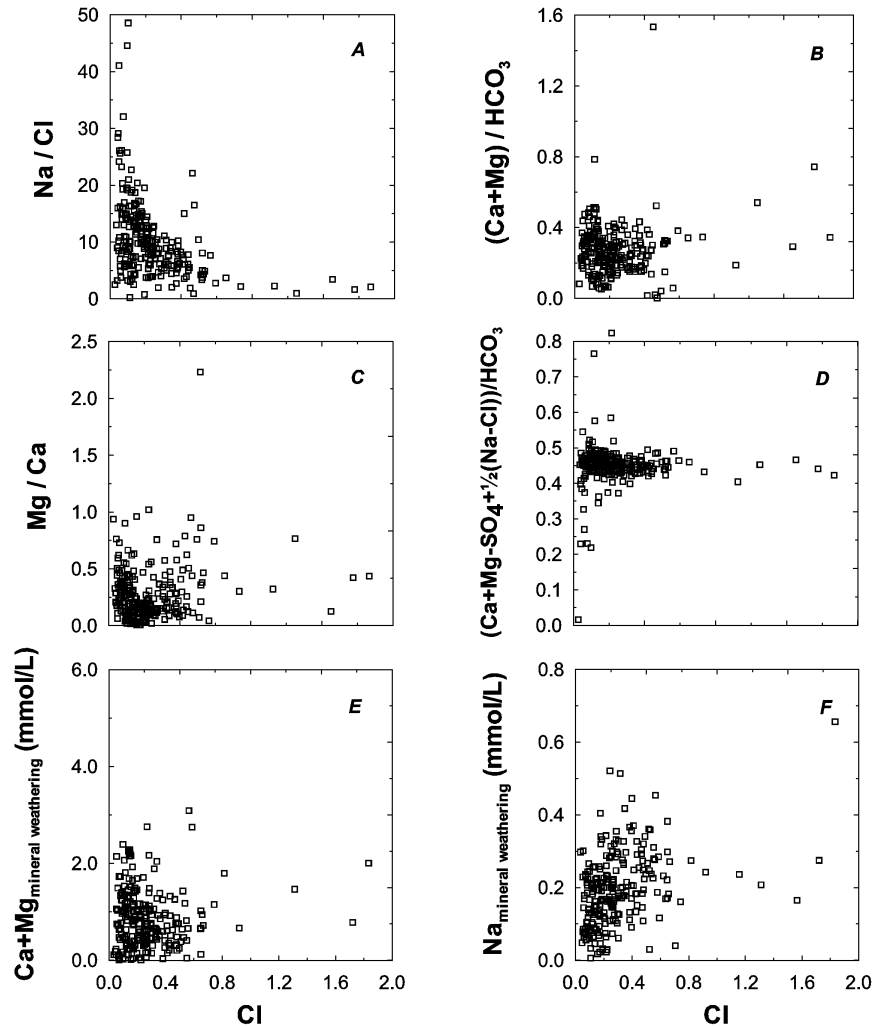
The  $[\text{Ca}+\text{Mg}-\text{SO}_4+1/2(\text{Na}-\text{Cl})]/(\text{HCO}_3^-)$  ratio examines the relationship between the calculated lithological calcium and magnesium component and bicarbonate by adding or subtracting calcium and magnesium originating from cation exchange ( $1/2(\text{Na}-\text{Cl})$ ) from calcium and magnesium of lithological origin ( $\text{Ca}+\text{Mg}-\text{SO}_4$ ). The lithological  $(\text{Ca}+\text{Mg})/\text{HCO}_3^-$  ratio is less than 0.5 (Fig. 11D). As weathering reactions of calcium and magnesium produce bicarbonate in a ratio of 1:2, there is an accessory source of bicarbonate. This indicates that albite and/or plagioclase weathering may take place.

**Table 2** Correlation coefficients between chemical major elements in groundwater. Bold letters indicate a significant correlation ( $p\leq 0.05$ )

	Na	Ca	Mg	K	Cl	SO <sub>4</sub>	NO <sub>3</sub>	SiO <sub>2</sub>	HCO <sub>3</sub>
Na		-0.28	-0.20	0.08	0.34	0.07	0.02	-0.06	<b>0.59</b>
Ca			<b>0.82</b>	0.17	0.23	<b>0.76</b>	0.04	0.01	0.41
Mg				0.12	0.30	<b>0.75</b>	0.06	0.01	0.40
K					0.31	0.12	0.01	0.42	0.27
Cl						0.33	0.11	-0.03	0.30
SO <sub>4</sub>							0.01	-0.14	0.26
NO <sub>3</sub>								0.10	0.05
SiO <sub>2</sub>									0.07



**Fig. 11** Ionic ratios to enlighten geochemical evolution of groundwater



## Dissolution Rates

### Ionic Ratio Calculations

From element concentrations it is possible to quantify dissolution rates in the aquifer which cannot be attributed to meteoric or cation exchange sources. Calcium and magnesium concentrations added to by the dissolution of calcite, dolomite and other minerals (anorthite, plagioclase, chlorite) show that weathering reactions contribute between 0.3 to 3.5 mmol/L of dissolved calcium and magnesium (Fig. 11E). At low salinities these represent about 80% of the total calcium and magnesium; however, the relative contribution drops to 50% with increasing salinity (Fig. 12A). Albite and plagioclase weathering, calculated as the difference between the lithological (Ca and Mg) and  $1/2 \cdot \text{HCO}_3$ , contributes less than 0.5 mmol/L of sodium (Fig. 11F). The meteoric-origin sodium contribution drops only slightly with increasing salinity from a maximum of about 9 to 8% (Fig. 12B). At low salinities the relative contribution of  $\text{Ca}^{2+}/\text{Na}^+$  exchange is nearly nonexistent; then it increases linearly with salinity up to 20%, while the predominant weathering-origin sodium

decreases from nearly 100% at low salinities to about 70% at high chloride concentrations.

Sodium from lithological sources is predominant in the aquifer geochemistry, increasing linearly with salinity up to some 4 mmol/L (Fig. 12C). The subsequent overall weathering reactions usually are lower than 2.5 mmol/L and increase only to some extent with salinity, which substantiates the slowness of weathering reactions of sediments in a crystalline-rock environment.

### Mass-Balance Calculations

The dissolution rates obtained from ionic ratios are compared with inverse geochemical modeling results of a few samples along three selected flow paths (Fig. 13). The geochemical program PHREEQC was used to determine the transfer rates between initial and final wells. The constraints used in the models were calcium, magnesium, sodium, potassium, carbon, sulfur, and silica (Table 3). The phases used were CO<sub>2</sub> (gas), calcite, dolomite, gypsum, chalcedony, kaolinite, albite, potassium feldspar, halite, and sylvite. Although chloride may be present in numerous minerals in small amounts (e.g. cotunnite PbCl<sub>2</sub>,

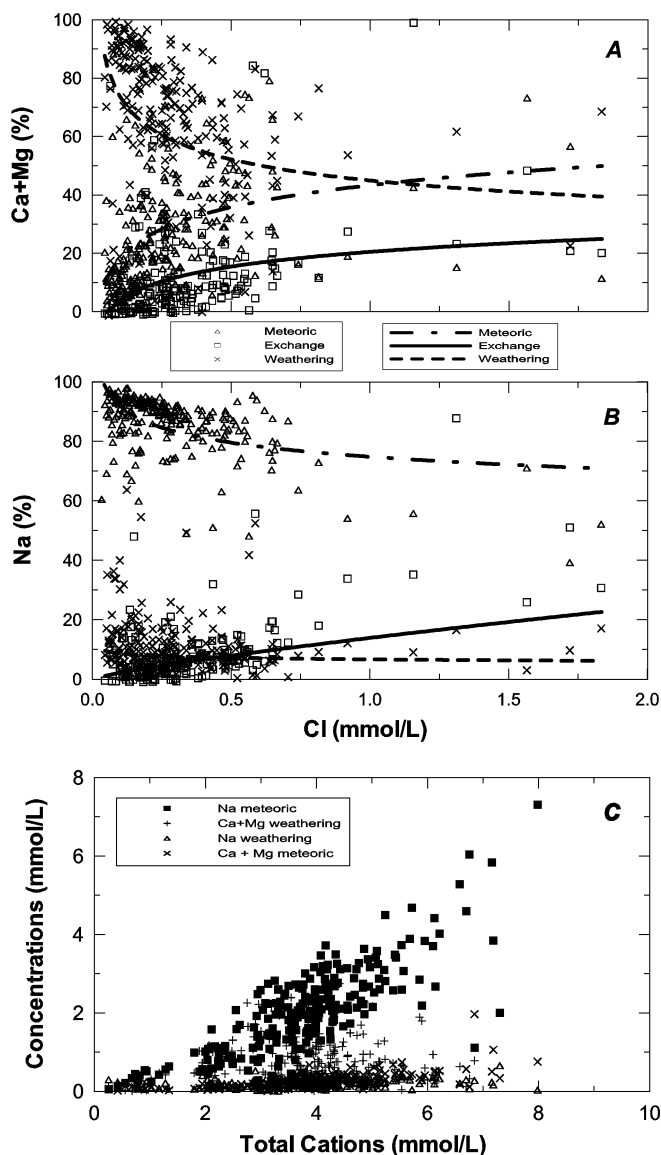


**Fig. 12** **A** Sources of Ca+Mg as percentage of the total concentration. **B** Sources of Na as percentage of the total concentrations. The three regression curves of each set are indicated. **C** Sources of dissolved cations with increasing total dissolved cations

matlockite  $\text{PbClF}$ , or phosgenite  $\text{PbCl}_2:\text{PbCO}_3$ , their occurrence, is rather exotic and their solubility lower than halite. Anorthite and K-mica minerals were only detected in volcanic rocks rich in alkalis (around San Miguel de Allende), although not in the selected flow paths. Quartz's kinetics are probably too low for the given  $\text{H}_4\text{SiO}_4$  content in groundwater from the study area. Silica is rather represented by chalcedony or amorphous silica. Soil samples from the discharge zones between San Miguel de Allende and Dolores Hidalgo indicate the presence of chalcedony (Mahlknecht 2001). Although sylvite is not an important constituent of the aquifer geochemistry of the study area and is only present in downgradient zones, it was added to the models because it accounts for potassium sinks. Hematite, a mineral which is frequently present in the aquifer,

was not considered in the modeling process due to uncertainty with respect to redox potential measurements. Ca-montmorillonite and kaolinite appear only in the granular aquifer in the center of the basin. In addition to the above-mentioned phases, the Ca/Na exchange option was added as a constraint. The cation exchange capacity (CIC) on selected samples in the entire study area showed that it is relevant in granular aquifer material ( $<20$  meq/100 g soil), but nearly nonexistent in the fractured aquifer material ( $<1$  meq/100 g) (Medina-Mejía 2003). Ornelas-Soto (2003) reported a maximum of 100 meq/100 g soil for soils in the San Miguel de Allende zone.

The flow path sections were selected along the main flow directions: a) San Felipe valley towards the basin's center (flow path A), San José Iturbide towards the basin's center (flow path B), and from the Sierra de Guanajuato towards Dolores Hidalgo (flow path C) (Figs. 1 and 13). Flow path A reflects the hydrochemical evolution from the unconfined western area of the Quaternary aquifer towards the semiconfined Tertiary conglomerates in the center of the basin. Sampling location RL-5 represents a natural spring with recharge from the Sierra de Santa Barbara. Flow path B reproduces the hydrochemical development from the felsic Zamorano massif in the southeastern part of the study area towards semiconfined to confined units in the center of the basin. Sampling location RL-8 represents a natural spring at the flanks of the Zamorano relief. Finally, flowpath C represents the evolution from the Sierra de Guanajuato to the semiconfined conditions near Dolores Hidalgo. Well RL-19 is a shallow well at the foot of the Sierra de Guanajuato. For all selected flowpaths it was assumed that mixture with other waters is negligible.

Table 4 illustrates the results obtained by successive modeling of sections between two sampling points. As can be seen, the majority of processes are dissolution oriented, which is in agreement with the corresponding saturation indices (Fig. 7, Table 3). Flow paths A and C obtain  $\text{CO}_2$  gas inputs throughout the entire cross section, while flow path B indicates conditions closed to  $\text{CO}_2$  in the downgradient segment (LS28-LS158). The open and closed  $\text{CO}_2$  conditions coincide well with the unconfined Quaternary sediments in flow paths A and C, and the trend from unconfined conditions in Quaternary sediments to semiconfined/confined conditions in Tertiary conglomerates and tuffs in flow path B, respectively (Fig. 13, Fig. 1).  $\text{CO}_2$  gas dissolution and calcite are the most important dissolution processes in unconfined zones (between 1.6 and 3.4, and 0.0 and 3.8 mmol/L, respectively), and exchange reactions predominate in confined zones (from 0.0 to 2.7 mmol/L for  $\text{Ca}^{2+}/\text{Na}^+$ , and from 0.0 to 1.8 mmol/L for reverse  $\text{Na}^+/\text{Ca}^{2+}$ ). Chalcedony and kaolinite precipitate at rates between 0.9 and 8.2 mmol/L, and 0.2 and 2.1 mmol/L, respectively. Elevated  $\text{CO}_2$  gas dissolution promotes albite weathering up to 3.7 mmol/L, which itself produces elevated chalcedony and kaolinite precipitation. Calcite may precipitate in low amounts in more evolved zones ( $<0.3$  mmol/L), whereas dolomite, gypsum and halite maintain dissolution tendencies along

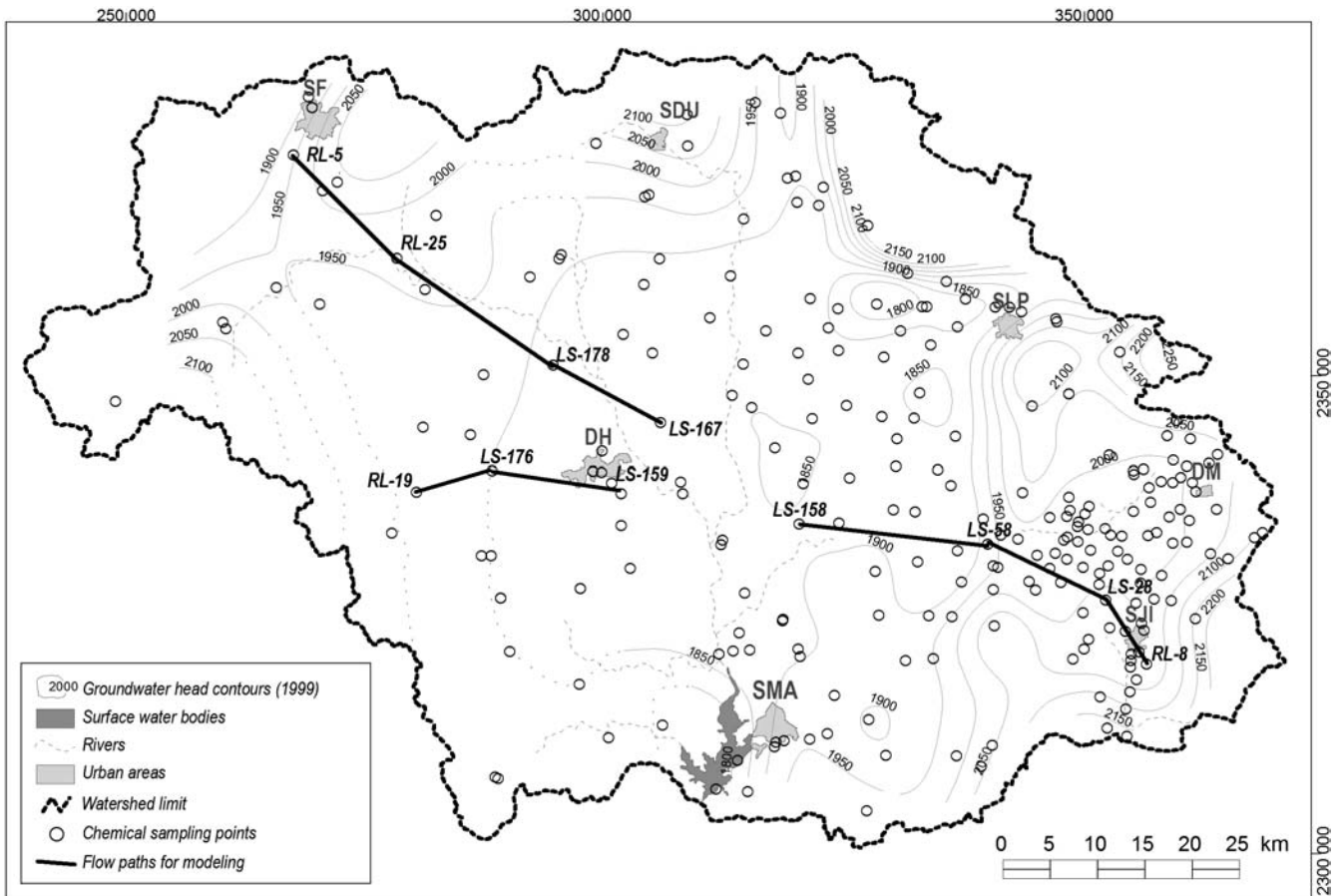


**Fig. 13** Map showing chemical sampling wells and springs, water-table contours (1999) and selected flow paths for mass balance modeling. Hydraulic head is given in meters above sea level

**Table 3** Data used in PHREEQC and corresponding calculated saturation indices; input data are given in mg/L, except for temperature (°C) and pH (standard units)

Sample ID	Temp	pH	HCO <sub>3</sub>	Ca	Mg	Na	K	Cl	SO <sub>4</sub>	SiO <sub>2</sub>	pCO <sub>2</sub>	SI <sub>calcite</sub>	SI <sub>dolomite</sub>	SI <sub>gypsum</sub>	SI <sub>halite</sub>
Flow path A															
RL-5	20.4	6.2	30.6	3.0	1.1	9.3	6.2	2.5	11.7	41.4	-1.7	-3.2	-6.6	-3.6	-9.2
RL-25	22.4	6.7	91.5	16.9	2.4	11.3	6.0	2.5	5.4	77.2	-1.8	-1.5	-3.5	-3.3	-9.1
LS-178	23.7	6.4	103.1	11.3	3.2	14.5	9.2	2.8	5.5	85.9	-1.4	-1.9	-4.0	-3.4	-8.9
LS-167	21.1	7.0	237.7	90.7	19.4	14.3	3.5	5.1	30.6	56.6	-1.7	-0.2	-0.8	-2.0	-8.7
Flow path B															
RL-8	20.4	6.0	27.5	3.4	1.5	6.6	4.9	2.7	12.4	42.4	-1.6	-3.4	-6.9	-3.5	-9.3
LS-28	28.7	7.3	234.9	15.5	0.9	71.8	9.8	4.3	12.1	43.3	-1.9	-0.5	-1.9	-3.0	-8.1
LS-58	29.5	7.3	251.6	36.6	3.5	48.5	18.2	7.7	17.2	92.5	-1.9	-0.1	-0.8	-2.6	-8.0
LS-158	29.6	7.4	285.0	34.9	2.5	72.1	22.3	8.9	35.0	99.0	-1.9	0.0	-0.8	-2.3	-7.8
Flow path C															
RL-19	22.8	6.3	60.8	6.8	1.4	13.5	3.7	1.6	4.4	56.4	-1.5	-2.5	-5.4	-3.7	-9.2
LS-176	21.4	7.0	175.1	23.4	8.0	27.0	13.2	10.6	8.2	88.9	-1.7	-0.9	-1.9	-3.0	-8.1
LS-159	28.8	7.3	285.2	47.1	2.9	67.8	17.4	17.2	39.7	118.4	-1.8	0.0	-0.8	-2.1	-7.5

most of the flow path trajectory (from 0.04 to 0.6, from 0.0 to 0.4 mmol/L, and from 0.14 to 1.9 mmol/L, respectively). K-feldspar dissolves from 0.0 to 0.4 mmol/L, while sylvite is absent in most segments. The precipitation of dolomite, in the order of 0.2 mmol/L in segment LS176-LS159, is thermodynamically unreliable and suggests that magnesite is the reactive magnesium carbonate rather than dolomite. Mineralogical investigations in this

zone, however, do not favor magnesium precipitation. This implies that different processes not considered in the models may be responsible (most probably mixing) for this flow path section. Amorphous silica dissolution rates are in the order 3 mmol/L and indicate that amorphous silica is reactive rather than chalcedony or quartz.

**Table 4** Mass transfer results for flow paths A and B (all data are in mmol/L H<sub>2</sub>O). model. "CO<sub>2</sub> (g)" means carbon dioxide gas, "CaX2" and "NaX" indicate the Na<sup>+</sup> for Ca<sup>2+</sup> exchange surfaces. Positive values indicate dissolution between initial and final water; negative values indicate precipitation. "-" indicates that the mineral phase is not included in the mass-balance

Flow path A	Model no.	CO <sub>2</sub> (g)	Dolomite	Calcite	Gypsum	K-feldspar	Albite	CaX2	NaX	Halite	Sylvite	Kaolinite	Chalcedony
RL5-RL25	1	0.42	0.05	0.40	-0.07	--	--	-0.04	0.07	--	--	--	--
	2	0.46	0.05	0.36	-0.07	--	0.07	--	--	--	--	-0.04	-0.14
	3	0.81	0.05	0.00	-0.07	--	0.79	0.36	-0.72	--	--	-0.40	-1.58
RL25-LS178	1	0.99	0.04	-0.08	--	0.08	--	-0.08	0.17	0.01	--	-0.04	-0.17
	2	1.07	0.04	-0.16	--	0.08	0.17	--	-0.33	0.01	--	-0.13	-0.50
LS178-LS167	1	0.56	0.62	--	0.28	--	--	0.16	--	0.22	-0.15	--	--
	1	2.33	0.59	0.90	0.24	--	--	--	-1.77	0.14	-0.07	--	--
	2	3.23	0.59	0.00	0.26	--	1.80	0.88	-1.77	1.94	-1.87	-0.90	-3.61
Flow path B RL8-LS28	1	3.23	0.59	0.00	0.26	--	1.80	0.88	-1.77	0.14	-0.07	-0.90	-3.61
	2	1.08	-0.03	1.71	Gypsum	K-feldspar	Albite	CaX2	NaX	Halite	Sylvite	Kaolinite	Chalcedony
	3	2.46	-0.03	0.32	--	0.12	--	-1.39	2.78	0.05	--	-0.06	-0.23
LS28-LS58	1	2.79	-0.03	--	--	0.12	2.78	--	--	0.05	--	-1.45	-5.78
	2	--	0.11	-0.25	0.05	0.12	3.42	0.32	-0.65	0.05	--	-1.77	-7.07
	3	0.48	0.11	--	0.05	0.21	--	0.62	-1.23	0.10	--	-0.11	-0.43
LS58-LS158	1	0.77	-0.04	0.22	0.19	0.10	--	0.42	-0.85	0.10	--	-0.11	-0.43
	2	0.59	-0.04	-0.19	0.19	0.10	--	-0.41	0.82	0.03	--	-0.05	-0.21
	3	1.61	0.04	--	0.19	0.10	0.99	--	--	0.03	--	-0.55	-2.18
RL8-LS158	1	2.93	0.04	1.83	0.24	0.44	0.62	-0.19	0.37	0.03	--	-0.36	-1.44
	2	3.44	0.04	0.51	0.24	0.44	--	-1.32	2.65	0.18	--	-0.22	-0.89
	3	0.50	0.27	0.00	0.24	0.44	2.65	--	--	0.18	--	-1.55	-6.18
Flow path C RL19-LS176	1	0.67	Dolomite	Calcite	Gypsum	K-feldspar	Albite	CaX2	NaX	Halite	Sylvite	Kaolinite	Chalcedony
	2	0.77	0.27	0.27	0.04	0.24	--	-0.17	0.33	0.25	--	-0.12	-0.49
	3	0.71	0.27	0.10	0.04	0.24	0.33	--	--	0.25	--	-0.29	-1.15
LS176-LS159	1	1.51	-0.21	1.27	0.33	0.11	--	-0.79	1.59	0.19	--	-0.39	-1.57
	2	1.98	-0.21	0.47	0.33	0.11	1.59	--	--	0.19	--	-0.05	-0.22
	3	1.21	0.06	--	0.33	0.11	2.54	0.47	-0.95	0.19	--	-0.85	-3.39
RL19-LS159	1	2.17	0.06	0.58	0.37	0.35	--	-0.96	1.92	0.44	--	-0.18	-0.70
	2	2.75	0.06	--	0.37	0.35	1.92	--	--	0.44	--	-1.14	-4.54
	3	0.58	0.06	--	0.37	0.35	3.08	0.58	-1.15	0.44	--	-1.71	-6.85



**Table 5** Comparison of transfer rates obtained from ionic ratio calculations and mass balance modeling. All data are given in mmol/L H<sub>2</sub>O. Negative values for cation exchange indicate reverse exchange

Geochemical Sources	Ionic ratio calculation	PHREEQC models							
		Entire study area		Flowpath A		Flowpath B		Flowpath C	
		Min	Max	Min	Max	Min	Max	Min	Max
Ca+Mg weathering	0.0–2.2	0.6	1.5	0.0	1.9	0.1	1.6		
Na weathering	0.0–0.4	0.0	1.8	0.0	3.7	0.0	3.1		
Ca+Mg meteoric	0.1–0.6	0.3	0.3	0.2	0.2	0.4	0.4		
Na meteoric	0.4–3.8	0.1	1.9	0.2	0.2	0.4	0.4		
Ca/Na exchange	0.0–0.3	-1.8	0.0	-1.0	2.7	-1.1	1.9		

**Comparison of Results**

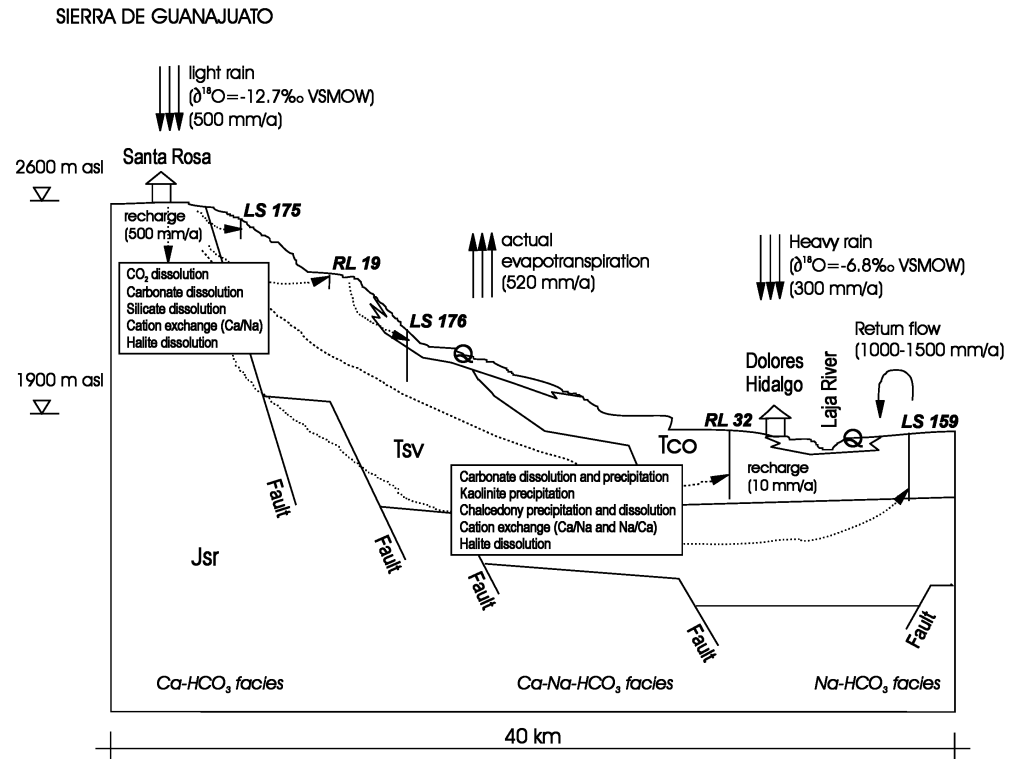
Both the mass balance approach and ionic ratio approach assign weathering of carbonates as the most important geochemical source for calcium and magnesium (up to 2.2 mmol/L) (Table 5). The contribution of meteoric calcium and magnesium is similar for both approaches (0.1 – 0.6 mmol/L). The range of exchange transfers according to ionic ratio calculations is from 0.0 to 0.3 mmol/L. Exchange rates according to mass balance rates vary between -1.8 (reverse Na<sup>+</sup>/Ca<sup>2+</sup>) and +2.7 mmol/L. A discrepancy between the mass balance approach and ionic ratio approach with regard to sodium sources is apparent: according to mass balance calculations, the meteoric sodium input is low (<0.4 mmol/L), while ionic ratios give meteoric sodium an important position (0.4– 3.8 mmol/L), whereas the same is not true with the ionic ratio method (<0.4 mmol/L). The difference between the two approaches is that the assumptions for the ionic ratio cal-

culaton are simpler, i.e. they do not consider CO<sub>2</sub> inputs and exchange in both directions (Ca<sup>2+</sup>/Na<sup>+</sup> and Na<sup>+</sup>/Ca<sup>2+</sup> option) while geochemical models reveal that CO<sub>2</sub> gas dissolution and reverse cation exchange are important processes. The additional CO<sub>2</sub> input promotes sodium weathering. Thus, the ionic ratio results overestimate meteoric processes, and underestimate sodium weathering processes which are calculated as residual from total transfers and from meteoric plus exchange transfers. In addition, mass balance models account for additional thermodynamic constraints (such as silica, potassium, pH, mineral phases, and saturation indices) and the calculations are done in sections which are open or closed to additional carbon sources. These additional constraints make the mass balance models more robust for geochemical evaluation.

**Recharge Conceptualization**

The results from isotopic and geochemical investigations are integrated into a conceptual model about recharge and subsequent geochemical evolution of the Independence

**Fig. 14** Schematic cross-sectional view of sources of recharge and hydrochemical evolution in the Independence basin (flow path C). Geological formations: *Jsr* Jurassic limestones; *Tsv* Tertiary volcanic sediments; *Tco* Upper Tertiary conglomerates; *Q* Quaternary sediments. Dotted lines and arrowheads indicate general direction of groundwater flow



Basin aquifer (Fig. 14). Groundwater of the Independence aquifer is of meteoric origin with an isotopic regression line similar to the regional meteoric water line. The infiltration is mostly via arroyos (wadis) and depressions with cyclic drying (November–May) and wetting (June–October). The recharge conditions have not changed during the last 10,000–13,000 years. Most rainwater infiltrates in the mountainous flanks of the northwestern (Sierra de Santa Barbara), southwestern (Sierra de Guanajuato) and southeastern (Zamorano massif) parts of the study area. In these areas, the infiltration rate may locally equal the precipitation rate (>800 mm). At the other extreme, there are very low infiltration rates (10 mm) in the plains of the northern Independence Basin (around San Diego de la Unión). Runoff passes through overland flow and tributaries to the main discharge (Laja River). The infiltration along this intermittent river and the Ignacio Allende dam is, however, most likely of minor importance for the overall recharge in the Independence Basin aquifer. The seepage of soil water through the unsaturated zone to the aquifer is slow enough to dissolve highly and less soluble salts.

During the infiltration process, CO<sub>2</sub> gas dissolution and carbonate weathering are predominant processes. The origin of calcium in groundwater is dissolution of calcite cement. Magnesium sources are from the weathering of dolomite/magnesite and gypsum. The sources of sodium are albite weathering and, to a lesser degree, halite dissolution. Exchange reactions are also a possible source for sodium. The source of chloride in groundwater is mainly from precipitation and irrigation return flow. Potassium is derived from feldspar (microcline) weathering. While calcite dissolution is the predominant process in unconfined recharge zones, it may be precipitated locally in the downgradient section of the flow paths. Silicate weathering is balanced out by silica/chalcedony and kaolinite precipitation. Normal Ca<sup>2+</sup>/Na<sup>+</sup> exchange is predominant, although reverse Na<sup>+</sup>/Ca<sup>2+</sup> exchange may take place locally.

## Conclusions

Stable isotopes of water and the hydrogeochemistry were utilized to understand the recharge mechanisms and geochemical evolution of groundwater in the Independence aquifer. The main conclusions are as follows:

Stable isotopes of groundwater indicate a distinct precipitation mechanism in the western and eastern parts of the Independence Basin. The <sup>18</sup>O-<sup>2</sup>H regression line of the eastern part agrees very well with the regional and world meteoric water line, whereas the groundwater of the Sierra de Guanajuato in the western part suggests a different precipitation origin/mechanism.

Enrichment of stable isotopes by evaporation in the western part implies an evaporative process occurring at or near the soil surface above the zero flux plane before deep percolation. Rapid infiltration can therefore be ex-

cluded for most of the rainwater. The evaporation is enhanced by recirculation caused by intensive irrigation.

After short rain events and irrigation periods, the water is completely consumed by evapotranspiration, and salt is precipitated. Large rainfall events or irrigation subsequently dissolve these salts and leach them slowly into the subsurface. The variations in groundwater salinity are relatively small. Increased salt contents (sulfate) in Mineral de Pozos (former mining area) can be attributed to mixing with deep confined groundwater from Cretaceous formations.

Cold waters show a δ<sup>18</sup>O variation of 6‰, which suggests that they are recharged by indirect infiltration with little mixing, preserving seasonal and elevation effects. Deep (warm to hot) groundwater δ<sup>18</sup>O values, by contrast, vary by less than 3‰ showing convergence at elevated temperatures toward a mean value of -10.1‰, which corresponds to the overall average of <sup>18</sup>O-δ-notation. The high degree of mixing correlates with longer flow paths and deeper circulation. However, isotope values from deep groundwater are indistinguishable from those of shallow groundwater. Thermal waters have the same stable isotope and geochemical signatures as the deep groundwater in the basin. Both shallow and deep waters receive recharge from highlands and summits, either inside of the basin or on the borders of the basin under similar climatic conditions.

Several mechanisms contribute to the subsequent chemical evolution of groundwater chemistry: CO<sub>2</sub> gas dissolution and carbonate weathering predominate in the unconfined flow sections. Other chemical processes adding calcium and magnesium are gypsum dissolution and cation exchange. The sources of sodium are primarily silicate weathering (albite) and exchange reactions on montmorillonite, kaolinite and hydroxide surfaces. Although ionic ratio calculations affirm the contrary, the meteoric sodium contribution (halite dissolution) is of minor importance. The source of chloride in groundwater is mainly meteoric. Potassium is derived solely from feldspar weathering. In the down-gradient confined areas, the main trend for carbonates is dissolution, although calcite may precipitate in small quantities.

The average recharge rate in the study area according to the CMB method, is 25 mm/year, having minima in the plains of the northern part (10 mm/year) and maxima in the southeastern highlands (>800 mm/year). The method suggests that in some zones there are additional chloride inputs from agriculture. The estimated recharge rates from shallow water of intensively cultivated farmlands in the northern part of the study area are thus possibly underestimated. A detailed analysis of additional inputs from the application of fertilizers and pesticides is necessary for obtaining accurate results.

**Acknowledgements** The University of Agricultural and Life Sciences (Universität für Bodenkultur Wien, BOKU Wien), Vienna, Austria, and the National Autonomous University of Mexico (Universidad Nacional Autónoma de México, UNAM), Mexico D.F., are thanked for the grants given to J.M. at the first stage of this investigation. Thanks are also due to “Programa de Mejo-

ramiento de Personal Académico – Universidad Autónoma de Nuevo León” for Ph.D. scholarship (I.N.L.). Access to relevant data and studies have been facilitated by the Consejo para el Desarrollo Regional Noreste (CODEREG Noreste) and the Comisión Estatal del Agua de Guanajuato (CEAG). Some of the analytical results used in this article were obtained during the project investigation under contract no. 02/16-CEAG/SDA/CONCyTEG-064, co-funded by CEAG, Consejo de Ciencia y Tecnología de Guanajuato (CONCyTEG) and Secretaría de Desarrollo Agropecuario (SDA). We are grateful to Dr. Margot Isenbeck-Schröter for her constructive comments on the manuscript.

## References

- Allison GB, Barnes CJ, Hughes MW, Leaney FWJ (1984) Effect of climate and vegetation on oxygen-18 and deuterium profiles and soils. In: IAEA Isotope hydrology 1983, Proc Symp, pp 105–123
- Allison GB, Hughes MW (1978) The use of environmental tritium and chloride to estimate total local recharge to an unconfined aquifer. *Aust J Soil Res* 16:181–195
- Arandá-Gómez JJ, McDowell FW (1998) Paleogene extension in the southern Basin and Range Province of Mexico: Syndepositional tilting of Eocene red beds and Oligocene volcanic rocks in the Guanajuato mining district. *Int Geol Rev* 40:116–134
- Birkle P, Torres Rodríguez V, Gonzalez Partida E (1998) The water balance for the basin of the valley of Mexico and implications for future consumption. *Hydrogeol J* 6(4):500–517
- Blaney HF (1959) Monthly consumptive use requirements for irrigation crops. In: Proc Am Soc Civil Eng, Div Irrigat Drain J 85 no. IR1:1–12
- Carrillo-Rivera JJ, Cardona A, Moss D (1996) Importance of the vertical component of groundwater flow: a hydrogeochemical approach in the valley of San Luis Potosí, Mexico. *J Hydrol* 185:23–44
- Carrillo-Rivera JJ, Clark ID, Fritz P (1992) Investigating recharge of shallow and paleogroundwaters in the Villa de Reyes Basin, SLP, México, with environmental isotopes. *Appl Hydrogeol* 4:35–48
- CEAG (2001) Piezometría Río Laja – San Felipe, Laguna Seca. Lluvias y Secas; September 1997–November 2000 [Piezometry of Río Laja-San Felipe, Laguna Seca. Rain and Dry seasons; September 1997 – November 2000]. Comisión Estatal del Agua de Guanajuato, Guanajuato, Mexico
- CEASG (1999) Actualización de modelos de disponibilidad hídrica superficial y subterránea en el Estado de Guanajuato [Actualization of the models of surface and groundwater availability in the Guanajuato State]. Comisión Estatal del Agua y Saneamiento de Guanajuato, Guanajuato, Mexico
- Clark ID, Fritz P, Quinn OP, Rippon P, Nash H, Bin Ghalib el Said B (1987) Modern and fossil groundwater in an arid environment. A look at the hydrogeology of Southern Oman. In: Use of stable isotopes in water resources development, IAEA Symposium 299, March 1987, Vienna, pp 167–187
- CNA (1992) Diagnóstico de las condiciones geohidrológicas actuales y de las alternativas de operación del acuífero de la cuenca alta del Río Laja, Estado de Guanajuato [Diagnostics of the actual geohydrological conditions and operation alternatives of the Cuenca Alta del Río Laja Aquifer, Guanajuato State]. Comisión Nacional del Agua, Mexico
- CNA (1995) Programa hidráulico 1995–2000 [Water program 1995–2000]. Comisión Nacional del Agua, Subdirección General de Programación, Mexico
- CNA (2000) El agua en México: retos y avances [Water in Mexico: objectives and advances]. Comisión Nacional del Agua, Subdirección General de Programación, México
- CODEREG (2000) Acuífero de la Independencia, municipios de San José Iturbide, Doctor Mora, San Luis de la Paz, Dolores Hidalgo, San Felipe, San Diego de la Unión y San Miguel de Allende [Independence Aquifer, municipalities of San José Iturbide, Doctor Mora, San Luis de la Paz, Dolores Hidalgo, San Felipe, San Diego de la Unión and San Miguel de Allende]. Consejo para el Desarrollo Regional Noreste y Norte, Guanajuato, Mexico, 107 pp
- Cortés A, Durazo J, Farvolden R (1997) Studies of isotopic hydrology of the Basin of Mexico and the vicinity: annotated bibliography and interpretation. *J Hydrol* 198:346–376
- Craig H (1961) Standard for reporting concentrations of deuterium and oxygen-18 in natural water. *Science* 133:1702–1703
- Daansgard W (1964) Stable isotopes in precipitation. *Tellus* 16:436–468
- Darling WG, Edmunds WM, Smedley P (1997) Isotopic evidence for paleogroundwaters in the British Isles. *Appl Geochem* 12:813–829
- Drever JI (1997) The geochemistry of natural waters: surface and groundwater environments, 3rd edn. Prentice Hall, New Jersey
- Edmunds WM, Carrillo JJ, Cardona A (2002) Geochemical evolution of groundwater beneath Mexico City. *J Hydrol* 258:1–24
- FAO-UNESCO (1988) Soil map of the world. FAO, Rome
- Ferrari L, López-Martínez M, Aguirre-Díaz G, Carrasco-Núñez G (1999) Space-time patterns of Cenozoic arc volcanism in central Mexico: From the Sierra Madre Occidental to the Mexican Volcanic Belt. *Geology* 27(4):303–306
- Gat JR (1980) The isotopes of hydrogen and oxygen in precipitation. In: Fritz P, Fontes J-Ch (eds) Handbook of environmental isotope geochemistry, vol 1. The terrestrial environment. Elsevier, Amsterdam, pp 21–47
- Gray DM (1973) Handbook of principles in hydrogeology. Water Information Center Inc., Huntington, New York
- Hoefs J (1997) Stable isotope geochemistry, 4th edn. Springer, Berlin Heidelberg New York
- Issar A, Gat J (1981) Environmental isotopes as tool in hydrogeological research in an arid basin. *Groundwater* 19(5):490–494
- Issar A, Quijano JL, Gat JR, Castro M (1983) The isotope hydrology of the groundwaters of central Mexico. *J Hydrol* 71:201–224
- Levin M, Gat JR, Issar A (1980) Precipitation, flood, and groundwaters of the Negev Highlands: an isotopic study of desert hydrology. In: IAEA arid zone hydrology: investigations with isotopic techniques, pp 3–23
- Mahlknecht J (2001) Química del agua subterránea en la Cuenca de la Independencia [Groundwater chemistry of the Independence Basin]. Internal Report, Institute of Geomatics and Hydraulics, University of Guanajuato, Mexico
- Mahlknecht J (2003) Estimation of recharge in the Independence aquifer, central Mexico, by combining geochemical and groundwater flow models. PhD Thesis, Institute of Applied Geology, University of Agricultural and Life Sciences (BOKU) Vienna, Austria, 296 pp
- Mazor E, Verhagen BT (1983) Dissolved ions, stable isotopes and radioactive isotopes and noble gases in thermal waters of South Africa. *J Hydrol* 63:315–329
- Medina-Mejía (2003) Un modelo Hidrogeoquímico del acuífero de San Miguel de Allende [A hydrogeochemical model about the aquifer of San Miguel de Allende]. Master thesis, Ciencias Básicas, Universidad Iberoamericana León
- Ornelas-Soto N (2003) Caracterización de la química y mineralogía de suelos y rocas en la zona de San Miguel de Allende [Characterization of the soil chemistry and mineralogy in the zone of San Miguel de Allende]. B thesis, Centro de Investigación en Química Inorgánica, Universidad de Guanajuato
- Parkhurst DL (1995) User's Guide to PHREEQC: a computer program for speciation, reaction-path, advective-transport, and inverse geochemical calculations. US Geol Surv Water-Resour Invest No. 95–4227
- Parkhurst DL, Appelo CAJ (1999) User's guide to PHREEQC (Version 2): a computer program for speciation, batch-reaction, one-dimensional transport, and inverse geochemical calculations: US Geol Surv Wat-Resour Invest Rep 99–4259, 310 pp
- Parkhurst DL, Plummer LN, Thorstenson DC (1982) BALANCE: a computer program for calculating mass transfer for geochemi-

- cal reactions in ground water. US Geol Surv Water-Resour Invest No. 82-14
- Payne BR (1988) The status of isotope hydrology today. *J Hydrol* 100:207-237
- Payne BR, Gaona S, García-Moreno C, Andrew B (1971) Estudio preliminar para la determinación de la relación entre aguas del Distrito de Riego No. 23 y las presas San Ildefonso y Constitución 1917. [Preliminary study for the determination of the relation between waters from the Irrigation district No. 23 and the San Ildefonso and Constitución 1917 dams]. OIEA-UNAM-INEN Internal Report. Mexico DF, 12 pp
- Plummer LN, Prestemon EC, Parkhurst DL (1991) An interactive code (NETPATH) for modeling net geochemical reactions along a flow path. US Geol Surv Water-Resour Invest No. 91-4078
- Remenieras G (1974) Tratado de hidrología aplicada [Treatise of applied hydrology]. Barcelona, Spain
- Rosenthal E (1987) Chemical composition of rainfall and groundwater in recharge areas of Bet-Shean-Harod multiple aquifer system. *Isr J Hydrol* 89:329-352
- Rozansky K, Araguas-Araguas L, Gonfiantini R (1993) Isotopic patterns in modern global precipitation. In: *Climatic change in continental isotopic records*. *Geophys Monogr* 78:1-36
- Rozansky K, Sonntag C, Munnich KO (1982) Factors controlling stable isotope of European precipitation. *Tellus* 34:142-150
- Sami K (1992) Recharge mechanisms and geochemical processes in a semi-arid sedimentary basin, Eastern Cape, South Africa. *J Hydrol* 139:27-48
- SARH (1981) Actualización del Estudio Geohidrológico de la Cuenca Alta del Río La Laja, Guanajuato [Actualization of the geohydrological study of the Upper Basin of River Laja, Guanajuato]. Secretaria de Agricultura y Recursos Hidráulicos, Dirección General de Aprovechamientos Hidráulicos, México
- Scanlon BR, Healy RW, Cook PG (2002) Choosing appropriate techniques for quantifying groundwater recharge. *Hydrogeol J* 10:18-39
- SCS (1964) Hydrology. SCS national engineering handbook. Soil Conservation Service, US Department of Agriculture, Washington DC, USA
- SPSS (1999) SPSS for Windows, release 10.0.1, SPSS, Inc
- UNESCO (1979) Map of the world distribution of arid regions. Paris MAB Tech Notes 7
- Winer BJ, Brown DR, Michel KM (1991) Statistical principles in experimental design. McGraw-Hill, New York, USA
- Wood WW (1999) Use and misuse of the chloride mass balance method in estimating ground water recharge. *Ground Water* 37(1):2-3
- Zhu C, Winterle JR, Love EI (2003) Late Pleistocene and Holocene groundwater recharge from the chloride mass balance method and chlorine-36 data. *Water Resour Res* 39(7):1182